Chapter 1

Introduction

1.1 Background

Strong demands for downsizing and lightweight of the mobile equipments accelerates development of highly integrated displays using low temperature poly-silicon (LTPS) thin-film transistors (TFTs) technologies. Various attempts have been reported to integrate display circuits to peripheral area of the glass substrate of the LCD, such as D/A converter, DC/DC converter, digital interface circuits and so on [1-2]. These technologies drastically reduce the number of the parts and allow simple module structure especially in mobile applications such as cellular phone and PDA.

In addition to these peripheral area integration, circuit integration to pixel is considered to be required to realize so-called high-value added display or sheet computer having input function. Integration of LTPS optical sensor is considered to have a potential to be a key technology for various kinds of advanced functions such as ambient light sensors, image scanners, artificial retinas, etc [3-4]. Figure 1-1 shows the system integration roadmap of LTPS TFT LCD.

1.2 Motivation

Reduction of power consumption through backlight control is one of the most important requirements for displays used in mobile applications. One way of achieving this is by sensing the ambient illumination conditions of the display. Under conditions of low ambient illumination the display brightness can be lowered saving power and reducing glare. Currently discrete photo diodes are used for most ambient

light sensing systems. Integration of light sensors reduces module complexity and location of the sensors close to the pixel array simplifies integration in products. There is an interest in integrating the sensors in the same LTPS technology used to fabricate the display so that the overall complexity of the module is reduced. Since the sensors are fabricated on the glass substrate using the same fabrication processes as conventional LTPS TFTs, fabrication costs can be saved [5-7].

A detailed analysis and full understanding of the effect of illumination on the LTPS TFTs electrical performances is necessary before the device can be used as a photo-sensor. In our research, we study on the feasibility of LTPS TFTs for light sensing application. First, we present an experimental study of the LTPS TFTs behavior under halogen lamp illumination. We have identified the different TFT operating regimes under illumination and have shown that the highest sensitivity to the illumination is obtained in the OFF-state. Furthermore, we propose a method to readout the photo-leakage current. A photo sensor is equipped with source follower, which converts photo-leakage current to analog voltage signal and buffers the converted voltage signal to analog-to-digital converter (ADC).

For practical usage, poly-Si TFTs are found to suffer from serious device variation behavior which results from the diverse and complicated grain distribution in the poly-Si film [8]. Therefore, it is very difficult to get a reliable sensing performance. Since the circuit performance changes with device variation, it will cause an error while sensing image. In this paper, we take further steps to estimate the influence from device variation on the sensing results, and try to calibrate the error.

1.3 Thesis Organization

Chapter 1 Introduction

1.1 Background

1.2 Motivation

1.3 Thesis Organization

Chapter 2 Photo Effect on Device

2.1 Fabrication Procedures of LTPS TFTs

2.2 Photo Effect of Front Light Illumination

2.3 Photo Effect of Back Light Illumination

2.4 Channel Width Effect

Chapter 3 Light-Sensing Circuit (LSC)

3.1 Introduction

3.2 Sensor Structure and Operation Principle

3.3 Source follower

3.4 Simulation and Experiment

3.4.1 Simulation

3.4.1.1 Simulated Method

3.4.1.2 Simulated Results

3.4.2 Experiment

3.4.2.1 Experimental Conditions & Results

3.4.2.2 Discussion about Experimental Results

3.4.3 Discussion about Simulated & Experimental Results

3.5 Digitization

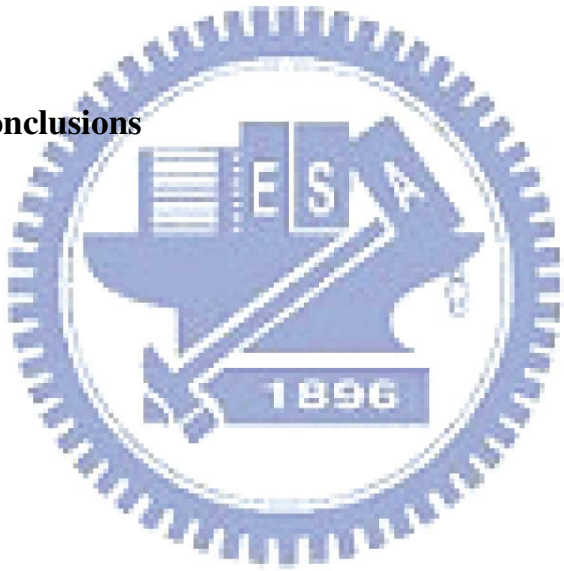

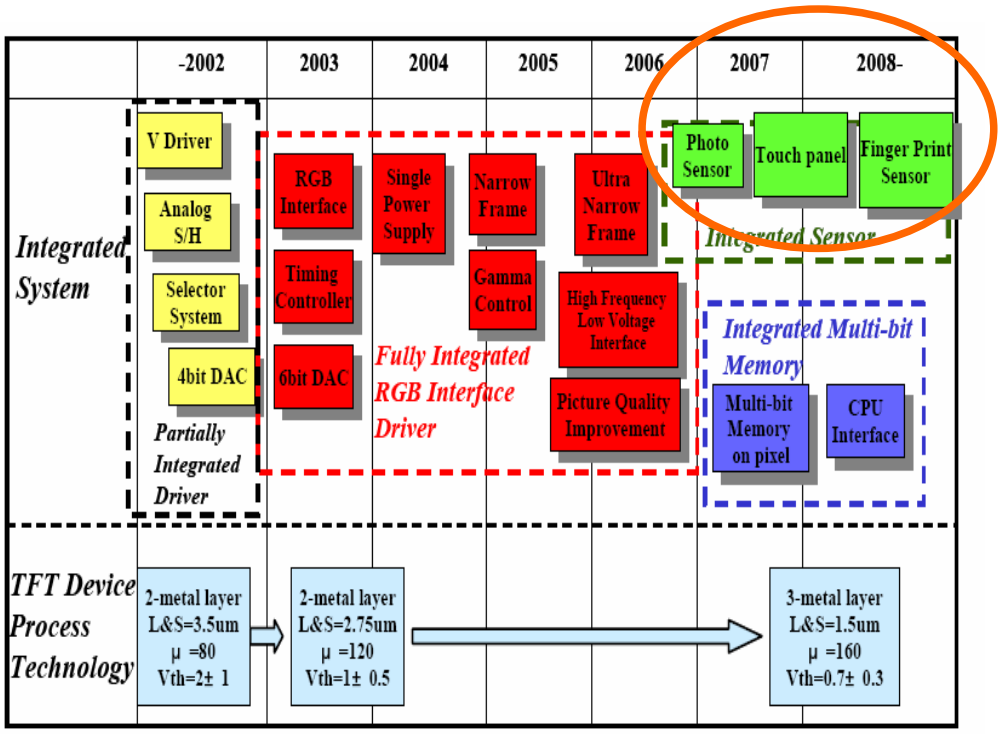

Figure 1-1 The roadmap from 2002 to 2008 (Ref. *Y.Nakajima et al.,SID' 06*)

Chapter 2

Photo Effect on Device

2.1 Fabrication Procedures of LTPS TFTs

In this study, the photo-sensor uses the identical LTPS TFTs fabrication on the glass substrate. The cross-section views of n-channel TFTs are shown in Fig 2-1. The basic process flow is described as follows. Firstly, the buffer oxide and a-Si:H films were deposited on glass substrates by the PECVD system. Then, XeCl excimer laser was used to crystallize a-Si:H film followed with poly-Si active area definition. Subsequently, gate insulator was deposited by PECVD. The thickness of gate oxide is 650Å. Next, the metal gate formation and source/drain doping were performed. Dopant activation and hydrogenation was carried out after interlayer dielectric deposition. Finally, contact holes formation and metallization were performed to complete fabrication work. The lightly doped drain (LDD) structure was used in the n-channel TFTs to generate photo leakage current (I_{photo}). The LDD length here is 2.5 μm, and width/length of the TFT is 20 μm/5 μm.

2.2 Photo Effect of Front Light Illumination

The typical transfer characteristics were measured both in the dark and under illumination of halogen lamp from the front side. Figure 2-2(a) and figure 2-2(b) show the LTPS TFTs transfer characteristics in the dark as well as irradiated at six different levels of halogen lamp illumination. For the three main TFT operating regimes, namely, ON regime, subthreshold regime, and OFF regime, the current level and photosensitivity are discussed.

To analyze in detail the photosensitivity, we have chosen V_{gs}=3V, 0.5V, -2V to bias device in the ON, subthreshold, and OFF regimes, respectively. We can observe a significant difference of the photosensitivity between these regimes, as seen in figure 2-3(a), figure 2-3(b) and figure 2-3(c). When TFT operates in the ON region, the drain current is almost independent of illumination intensity. In subthreshold region and OFF region, we can see the photosensitivity is significantly higher than that in the ON-state, especially in the OFF-state. For further discussion, we define the ratio of the TFT drain current under illumination (I_{D_illum}) to that in the dark (I_{D_dark}) as $R_{L/D} = I_{D\_illum} / I_{D\_dark}$ [9]. Figure 2-4 shows the comparison of the $R_{L/D}$ under illumination and in the dark and the current level is shown in its inset among ON, subthreshold, and OFF region. Although the current level of ON-state is 5 to 6 orders larger than the others, TFT has poorer $R_{L/D}$ in the ON-state than those in the subthreshold and OFF-state. In the aspects of photosensitivity, ON regime is not suitable for the light sensing application, but it is suitable for being the readout part. For this reason, only the behaviors of subthreshold region and OFF region in the later sections are considered.

2.3 Photo Effect of Back Light Illumination

In order to integrate the photo-sensor into the pixel [10-11], we should consider the photo effect of back light (BL) illumination to simulate its real situation on panel. The illumination sources for this measurement were halogen lamp from front side and LED white light from back side (figure 2-1). A comparison of TFT transfer curves for front and back side illumination are shown in figure 2-5(a) and figure 2-5(b). We can see on these figures the drain current of BL illumination (3940 lx) is approximately equivalent to the current of fourth front light (FL) illumination intensity (9113 lx).

Under BL illumination, the whole active layer include n^+, n^-, and intrinsic were illuminated. Consequently, in case of under the same illumination intensity (3940 lx), the effect on I_{D_BL} is greater than that on I_{D_FL}.

In addition, illuminating the device with FL and BL at the same time, it seems that the effects of BL and FL on the drain current can be added as shown in the insets of figure 2-5(a) and figure 2-5(b). When the FL illumination intensity is smaller than 1000 lx, the drain current is 1 to 2 orders of magnitude smaller than the current under BL illumination. There is no obvious increase of drain current till the FL intensity was larger than BL intensity. Figure 2-6(a) and figure 2-6(b) show the I_D-V_D characteristics of subthreshold and OFF region under FL and BL illumination and in the dark circumstance, respectively. We can observe more clearly in these figures, the effects of BL and FL on the drain current can be added. To further discuss on the photo effect of back light illumination, the off current and subthreshold current versus the FL intensity are plotted in figure 2-7(a) and figure 2-7(b), respectively. Also, with the FL equivalence of BL, the corresponding curves for the case of BL are plotted in their insets. When we illuminate the device with FL and BL at the same time, the BL intensity can be equivalent as FL intensity 5481 lx in OFF region and 8276 lx in subthreshold region. Therefore, the drain current result from FL and BL could be shift 5481 lx in OFF region and 8276 lx in subthreshold region. However, the equivalent quantity of shift in OFF region is not the same as that in the subthreshold region. We think there is something different when BL illuminated the whole active layer in the OFF region and subthreshold region. If we only want to eliminate the BL effect during the sense period, this issue might not so important. In such a case, the photo effect of BL illumination in this thesis is subsided.

2.4 Channel Width Effect

The dependence of I_{photo} (I_{D_illum}- I_{D_dark}) on channel width (W) is shown in figure 2-8. Channel length (L) of TFTs to measure W dependence is 5 μm. I_{photo} is proportional to W, as expected, both in subthreshold region and OFF region. Anyway, referring to the previous reports, Kobayashi *et al*. the I_{photo} is not strongly dependent on L for L > 2.5μm. It is thought that I_{photo} is generated uniformly in the W direction, but generated non-uniformly in the L direction. That is, I_{photo} is generated in a limited region between the source electrode and the drain electrode [12].

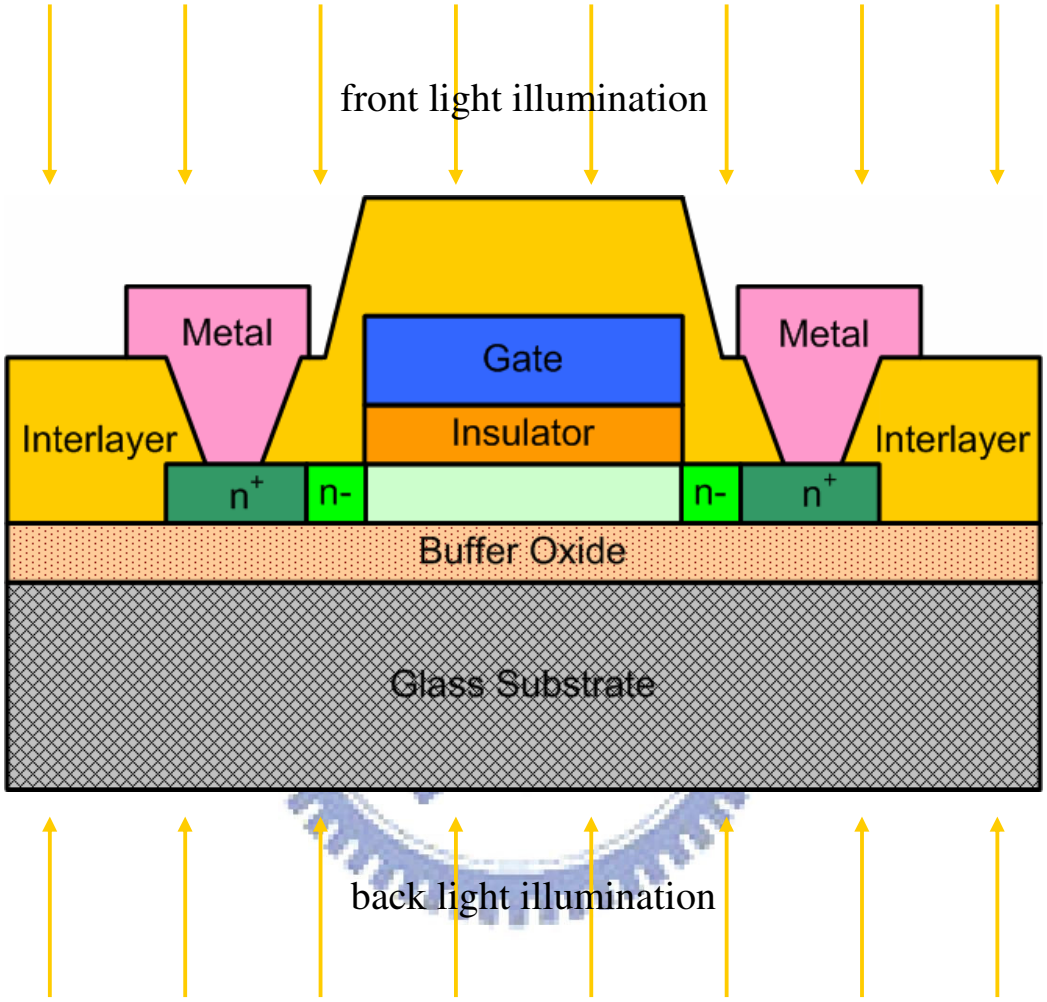

Fig. 2-1 The cross-section views of N-channel LTPS TFTs with LDD structure

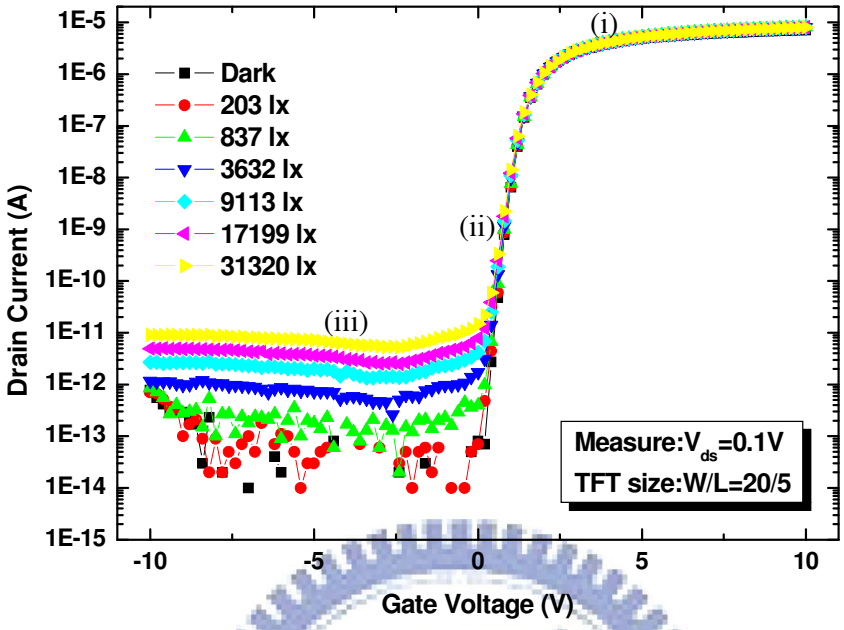

Fig. 2-2(a) LTPS TFT transfer characteristics in the dark and under illumination at V_{DS}=0.1V including regions (i) ON (ii) subthreshold (iii) OFF

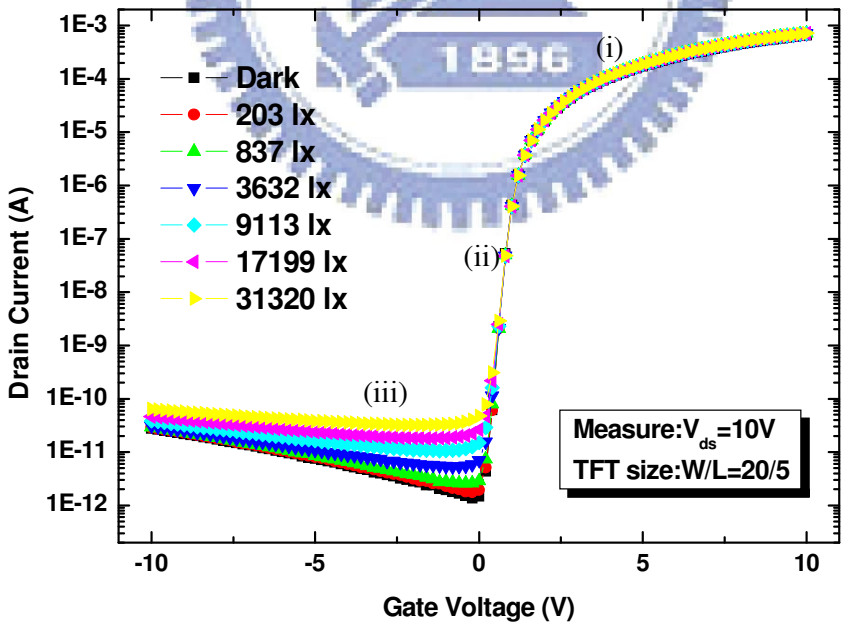

Fig. 2-2(b) LTPS TFT transfer characteristics in the dark and under illumination at V_{DS}=10V including regions (i) ON (ii) subthreshold (iii) OFF

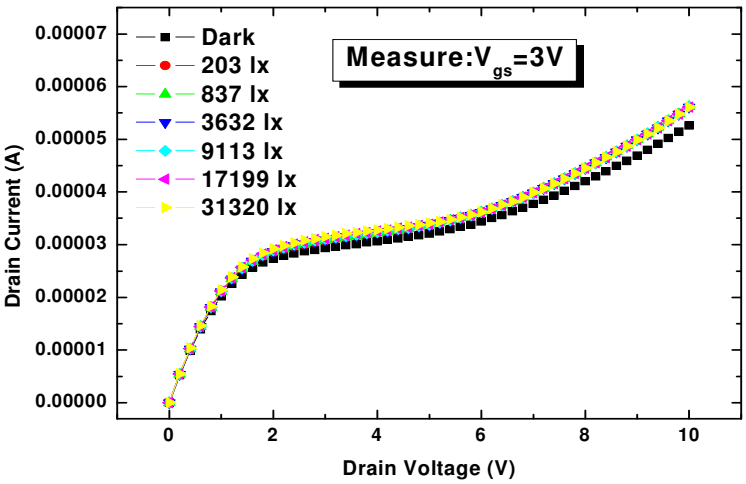

Fig. 2-3(a) ID-VD characteristics of ON region in the dark and under illumination

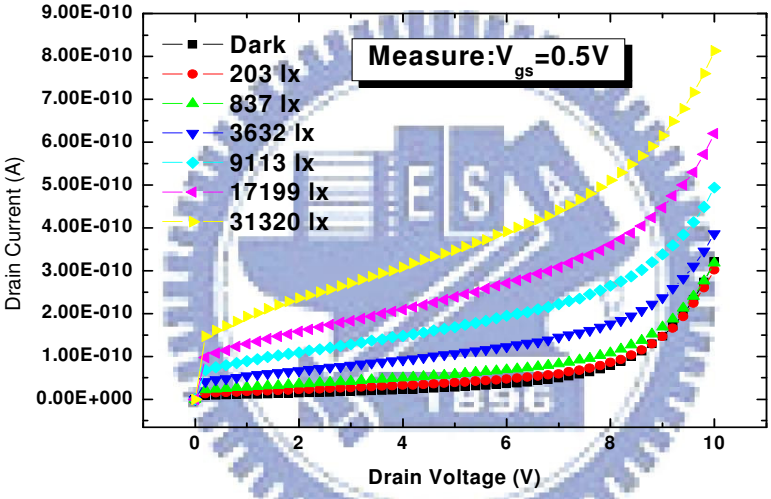

Fig. 2-3(b) ID-VD characteristics of Sub. region in the dark and under illumination

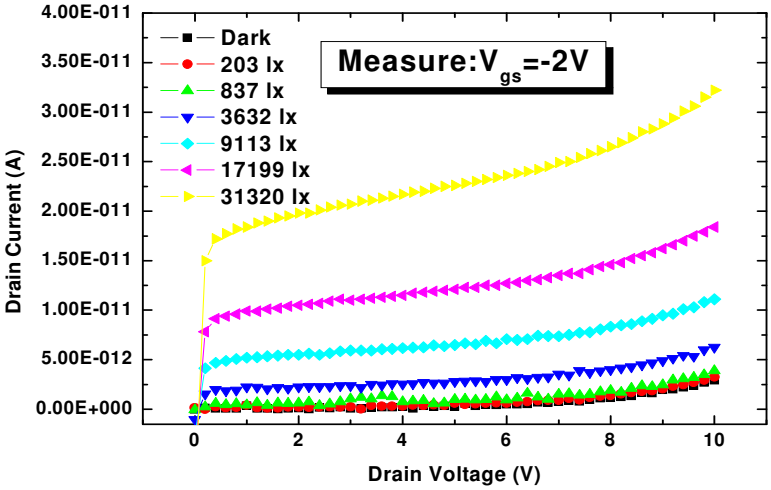

Fig. 2-3(c) ID-VD characteristics of OFF region in the dark and under illumination

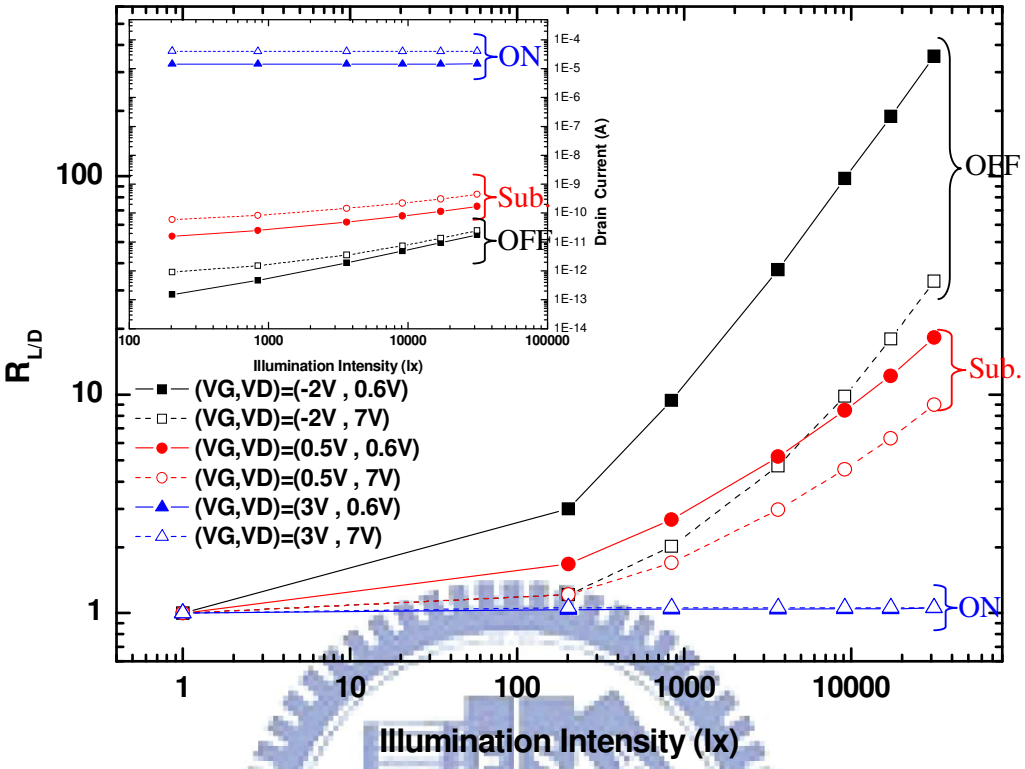

Fig. 2-4 The comparison of the $R_{L/D}$ under illumination and in the dark among ON, subthreshold, and OFF region and that of current level (inset)

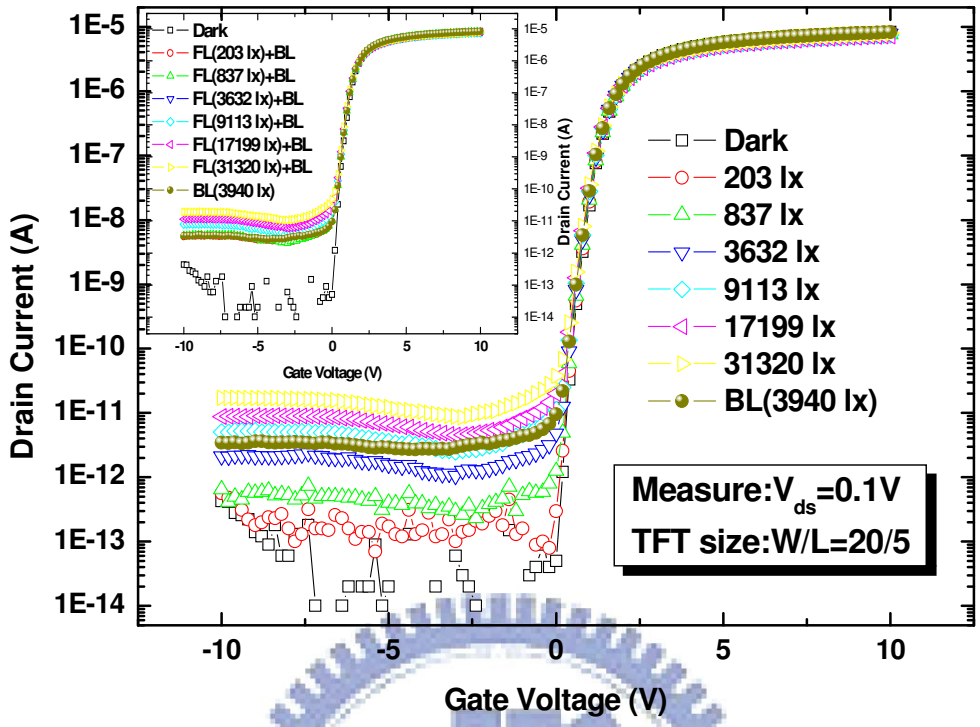

Fig. 2-5(a) LTPS TFT transfer characteristics in the dark and under FL and BL illumination at V_{DS}=0.1V

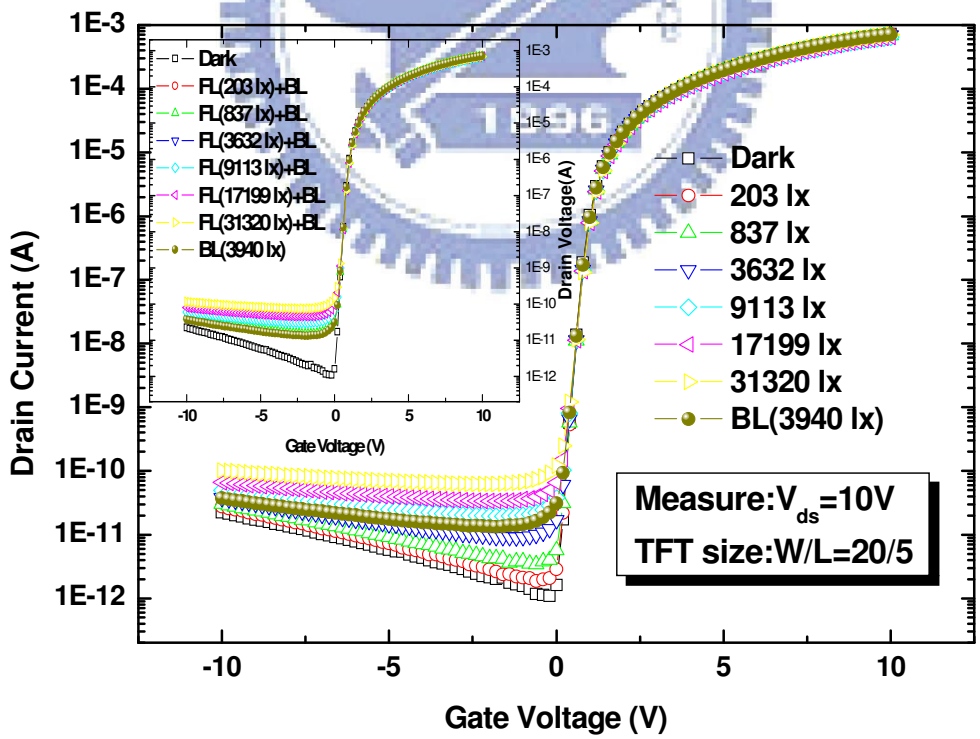

Fig. 2-5(b) LTPS TFT transfer characteristics in the dark and under FL and BL illumination at V_{DS}=10V

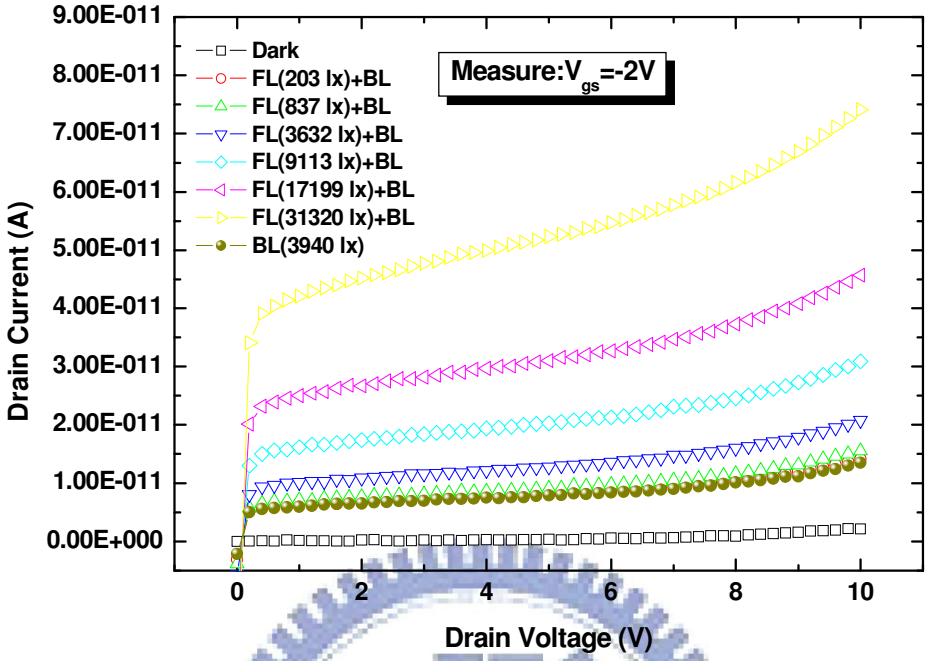

Fig. 2-6(a) I_D-V_D characteristics of OFF region in the dark and under FL and BL illumination

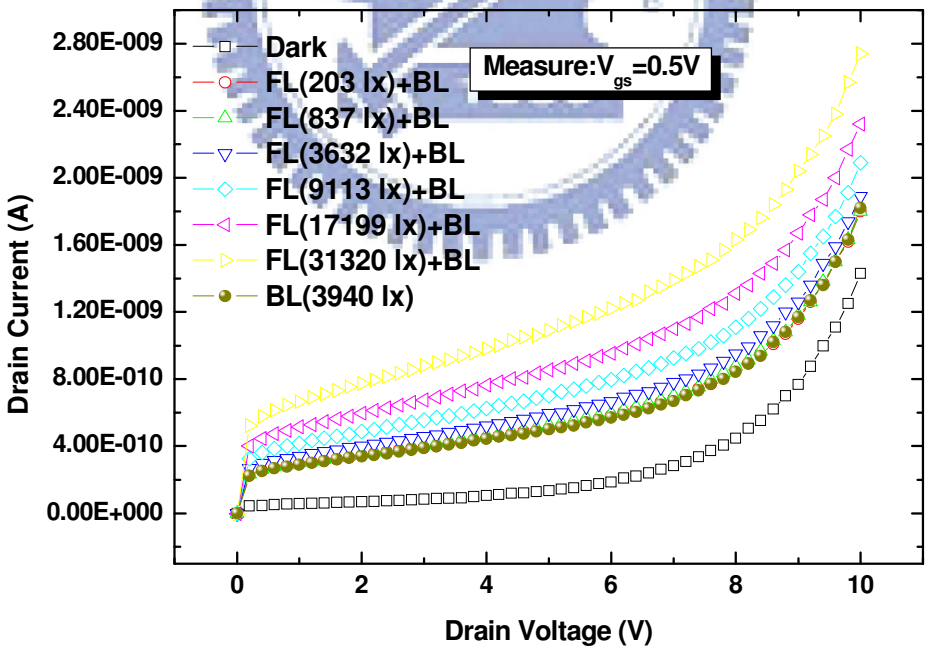

Fig. 2-6(b) I_D-V_D characteristics of Sub. region in the dark and under FL and BL illumination

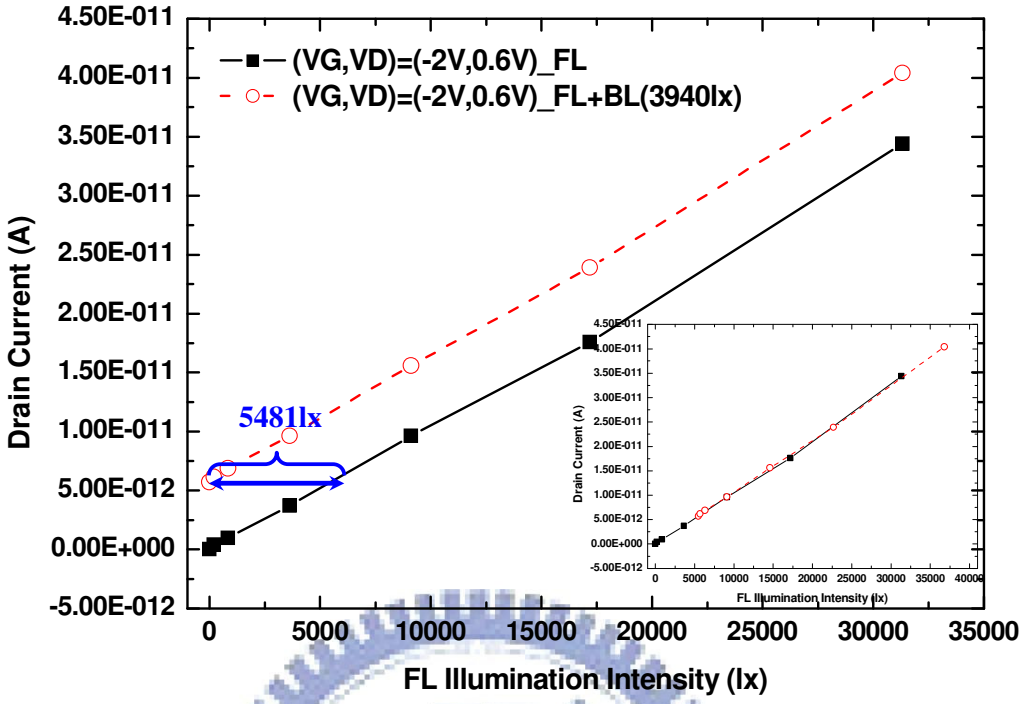

Fig. 2-7(a) The OFF current versus FL illumination intensity

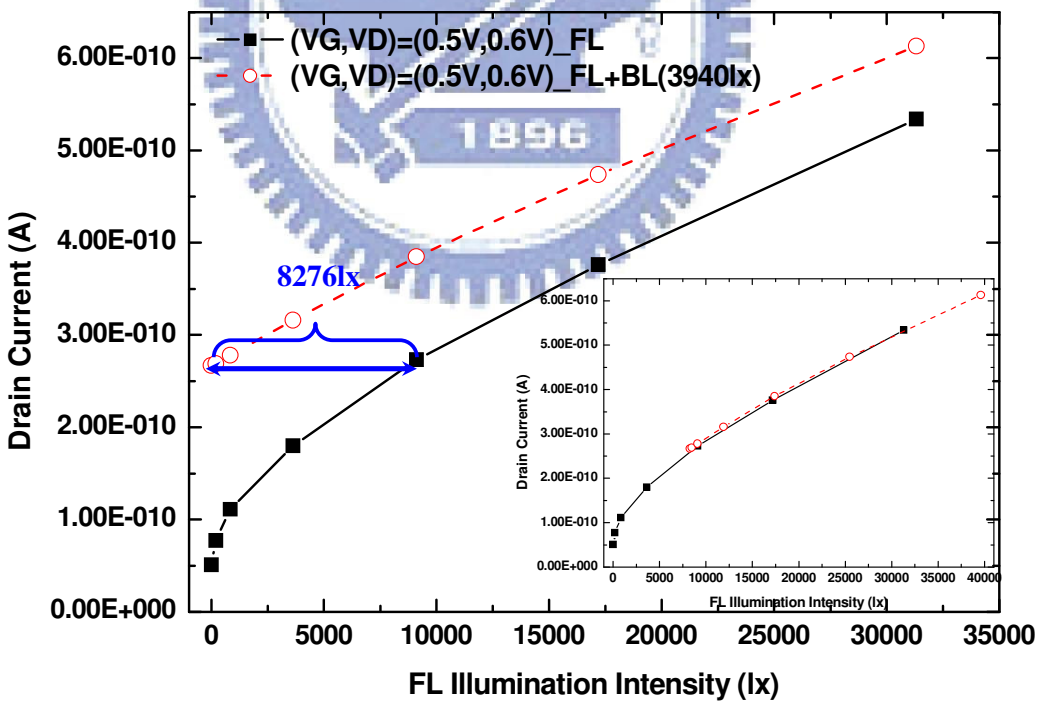

Fig. 2-7(b) The subthreshold current versus FL illumination intensity

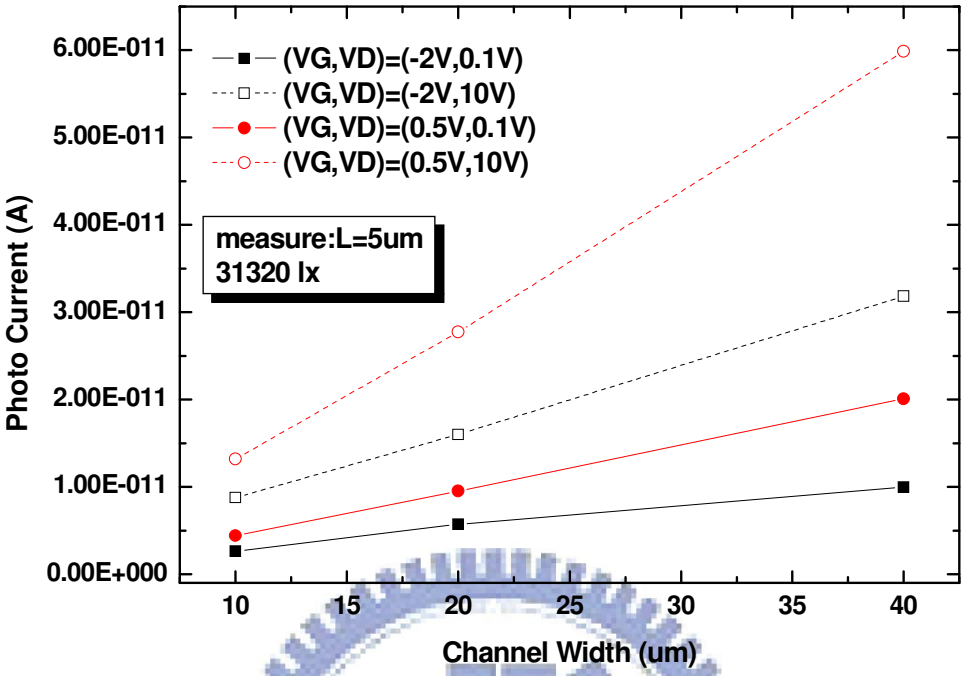

Fig. 2-8 Dependence of I_{photo} on channel width (W)

Chapter 3

Light-Sensing Circuit (LSC)

3.1 Introduction

Generally, the ambient light sensing function has been implemented using an additional chip or several components in the display module for mobile applications [13]. However, there are problems associated with the increase in the volume of the display module and difficulties in the manufacturing of the display module that allows light to be guided to the chip. On the other hand, if an ambient light sensing circuit is integrated to the panel even the pixel using LTPS TFTs, this can both decrease the display module volume and lower the manufacturing cost.

Because the ambient light sensing device is fabricated using thin-film technology and crystallization process, the detection area, the LDD, is very thin. Moreover, the photo current of LTPS TFTs is lower than that of the photodiode used in complementary metal oxide semiconductor (CMOS) image sensor (CIS). It is very difficult to design a readout circuit that performs very sensitively to readout such small photo leakage current. Therefore, we proposed a light sensing circuit that can convert photo leakage current to analog voltage signal and buffer the converted voltage signal to analog-to-digital converter (ADC). Measurements using the proposed light sensing circuit are performed to verify the performance of the proposed circuit.

3.2 Sensor Structure and Operation Principle

After the discussions about illumination effect of LTPS TFTs in chapter 2, we try to operate the device in the subthreshold [14] and OFF region under both ambient light and dark circumstances. Because the drain current of TFT is proportional to the illumination intensity, we proposed a circuit to sense the drain current under illumination and in the dark. Figure 3-1(a) and figure 3-1(b) show the schematic of the proposed 1T1C light-sensing circuit and its timing sequence, respectively. The proposed circuit consists of a storage capacitor (C_S) and a LTPS TFT (T1), which channel width is 400 μm and length is 8 μm, as the sensing device. In order to observe the signal easily, we enlarged the channel width to increase the photo leakage current level of our sensing device.

The operating principles can be described as two periods shown in the timing diagram. In the charge period (1), when gate signal becomes "high", T1 TFT is turned on. Thereby, the input voltage (V_{in}) "high" is stored in C_s and the voltage of node A (V_A) is charged to "V_{in_high}". In the discharge period (2), the gate voltage of T1 is applied so that T1 is operating in the subthreshold or OFF region while sensing operation. At the same time, V_{in} becomes "low". The photo leakage current, which is determined by the intensity of the ambient light, drained away through the T1. And the V_A, which is held by C_s, is discharged by the photo leakage current of T1.

However, there is a serious problem in measurement. We can not probe out the signal of node A if we want to know the V_A immediately. Because of the photo leakage current will drain away through the probe of oscilloscope, we need to convert the photo leakage current to analog voltage signal. There are several ways to achieve this purpose, and the most common method is using an operational amplifier (OP-Amp) [15-16]. However, an OP-Amp using LTPS TFTs needs many transistors,

which occupy a large area and increase cost. In order to integrate the sensor into pixel, using an OP-Amp seems not a good method. Hence, we added a TFT (T2) to be a source follower readout part [17] as shown in figure 3-2(a) and figure 3-2(b). A 2T1C light-sensing circuit and its timing sequence have been proposed.

3.3 Source Follower

We have to discuss the electrical characteristics of the source follower before the operation of the 2T1C light-sensing circuit. A conventional source follower is shown in figure 3-3(a). The ideal transfer characteristic of the conventional source follower can be expressed as

$$V_{out} = V_{in} - V_{th}. \quad (1)$$

Because the signal we measured at node A in discharge period is similar to a triangular wave (figure 3-1(b)), we used a triangular wave as input signal for the source follower testing. Figure 3-3(b) and figure 3-3(c) show the wave form and frequency response of output signal when the input triangular signal is 2V to 9V. We can see the output waveform will distortion when the input frequency exceeds 100Hz. For this reason, the maximum operation frequency of the signals of the sensing circuit will be limited to 100Hz.

Moreover, the circuit we proposed is used to sense the drain current in illuminated and dark conditions. We need to analyze the photo effect of the source follower. The input and output wave forms under illumination (31320 lx) and in the dark are shown in figure 3-4(a) and figure 3-4(b). There is no difference between illumination and dark; this is all because the source follower was operated in the ON region. As we discussed above, the photo current was almost independent of illumination intensity when TFT operated in ON region.

3.4 Simulation and Experiment

We have discussed the electrical characteristics and illumination dependence of T2 TFT which operates as a source follower in the sensing circuit. Because the source follower was operated in the ON region, there is no difference between illumination and dark. Therefore, due to the T1 TFT is the sensing device in the circuit, it is necessary to figure out the characteristics of the T1 TFT both in the illuminated and dark conditions.

3.4.1 Simulation

For proposed 2T1C light-sensing circuit as mentioned in the section 3.2, it is necessary to simulate the behaviors of our light sensor before practical usage.

3.4.1.1 Simulated Method

In the RPI models of TFT, there is no photo leakage current model for SPICE simulation [18], so we can not simulate the photo leakage current under different illumination directly. We have to modify the simulation method according to illuminated characteristics of device. Figure 3-5 shows the illumination dependence of I_D-V_D characteristics curve; the drain current increased while the illumination intensity enhanced. We selected the approximately linear region of the I_D-V_D curve to fit the formula, which can be expressed as

$$I_D = I_0(L) + A_0(L) \cdot V_D \ , \tag{2}$$

where $I_0(L)$ and $A_0(L)$ are intercept and slope, which are illumination dependence. Therefore, we use the different current sources and resistances parallel to represent the different photo leakage currents of TFT. Table 3-1 shows the values of $I_0(L)$ and $R_0 = 1/A_0(L)$ at V_{gs}=0.5V with the illumination intensity variation. When the illumination intensity changes, the value of $I_0(L)$ and R_0 change with it.

3.4.1.2 Simulated Results

Figure 3-6 shows the SPICE simulation results of TFT (W/L=20um/5um), we added a current source $I_0(L)$ and a resistance R_0 parallel to simulate the photo leakage current as shown in its inset. In this figure, we can see the results already can represent the photo leakage current. Consequently, we have figured out a method to modify the simulation model. Figure 3-7(a) and figure 3-7(b) show the modified 2T1C light-sensing circuit model for simulation and its time diagram. We can simulate the situations of TFT under illumination and in the dark by this model. The simulation results are shown in the figure 3-8. We can see in this figure, as expected, the output voltage (V_{out}) is discharged by the photo leakage current of T1. The larger the illumination intensity, the faster the discharge rate are. Its response time is around several mini seconds.

3.4.2 Experiment

3.4.2.1 Experimental Conditions and Results

The proposed 2T1C sensor has been fabricated on the glass substrate using LTPS technology for verification of light-sensing operation and the output characteristics as shown in figure 3-9. The experimental conditions are summarized in Table 3-2. Because the proposed sensor must operate with the display panel, we have to read out the output signals during the operation frequency of the display panel, 60 Hz (16.7ms). The operation frequencies of subthreshold and OFF region that we chose are 100 Hz and 10 Hz, respectively. The output voltage of the proposed circuit is measured by oscilloscope during discharge period under halogen lamp illuminative variations from 0 to 31320lx, and its waveforms are shown in figure 3-10(a) and figure 3-10(b). The discharging rate of V_{out} which is due to photo leakage can be expressed as *dV/dt*. Consequently, the slopes (*dV/dt*) of the waveforms can reflect the subthreshold or

OFF current under illumination and in the dark by the equation as following:

$$I_{D\_illum} = C_S \cdot (\frac{dV_{out}}{dt}). \quad (3)$$

It is like a constant current, so that the illumination intensity can be sensed.

3.4.2.2 Discussion about Experimental Results

However, in the discharge period (2) as discussed in section 3.2, the photo leakage current drained away through the T1. At the same time, the V_A drops to "V_{in_low}" with time. We can see in figure 3-5, the drain current varies as the drain voltage changes. Hence, we have to verify the accuracy of the function of the circuit. The full well capacity or saturation charge Q_{sat} is given by:

$$Q_{sat} = C \cdot V = I \cdot t, \quad (4)$$

from equation (2), an ordinary differential equation of V_A can be expressed as

$$I_0(L) + A_0(L) \cdot V_A(t) = C_S \cdot \frac{dV_A(t)}{dt}. \quad (5)$$

After solving the equation, we can get:

$$V_A(t) = \alpha \cdot e^{\frac{A_0(L)}{C_S} \cdot t} - \frac{I_0(L)}{A_0(L)}. \quad (6)$$

Expanding equation (6) by Taylor series:

$$V_A(t) = \alpha \cdot [1 + \frac{A_0(L)}{C_S} t + \frac{1}{2}(\frac{A_0(L)}{C_S} t)^2 + \cdots] - \frac{I_0(L)}{A_0(L)}, \quad (7)$$

because of our design,

$$\frac{A_0(L)}{C_S} << 1 \text{ and } \alpha = V_A(0) + \frac{I_0(L)}{A_0(L)},$$

where $V_A(0)$ is the initial voltage "V_{in_high}" during discharge period. Therefore, equation (7) can be simplified as

$$V_A(t) = V_A(0) + [\frac{I_0(L)}{C_S} + \frac{A_0(L)}{C_S} \cdot V_A(0)] \cdot t \,. \quad (8)$$

Equation (8) shows that the *dV/dt* only depends on illumination intensity. From equation (1) we know that

$$V_{out}(t) = V_A(t) - V_{th} \,. \quad (9)$$

Therefore, we can rely on calculating the slope of the waveforms to reflect the subthreshold or OFF current under illumination and in the dark. Then, the illumination intensity can be sensed by equation (3), as shown in figure 3-11.

3.4.3 Discussion about Simulated and Experimental Results

As the figure 3-8 and figure 3-10 shown, we can see the response time is around 3 mini seconds in the simulated results as well as in the experimental results when TFT operated in the subthreshold region. In the OFF region, the response time is around 10 mini seconds. We take further steps to compare the accuracy of the simulated results with the experimental results. Figure 3-12 shows the comparison with simulated and experimental results at V_{gs}=0.5V. The fitting formula (dash line) is expected to be a line which passes through the origin and its slope is equal to 1. However, the actual fitting formula is not as we expected. It does not pass through the origin and has a 17% error in the slope. The intercept may be comes from the threshold voltage difference when we modified the simulation model as well the error in the slope comes from the device variation. Therefore, it is a big issue to consider the device variation and we will discuss it in the next chapter.

3.5 Digitization

In order to restrain the interference of noise and avoid the error due to V_{th} shift of source follower, a high accuracy ADC has been proposed. The digitization circuit is shown in figure 3-13(a), which consists of two comparators, a "AND" logic gate and a counter. Two reference voltages V_{ref_1} and V_{ref_2} are used to compare with V_{out}, we can adjust the range of V_{out} with different signals "V_{ref_1}" and "V_{ref_2}". If $V_{out} > V_{ref\_1} > V_{ref\_2}$ or $V_{ref\_1} > V_{ref\_2} > V_{out}$, the output of logic gate C is always "0", as shown in figure 3-13(b). Only when $V_{ref\_1} > V_{out} > V_{ref\_2}$, the output of logic gate C will be the clock numbers of CLK. Therefore, we can discriminate the slopes of V_{out} between different illumination intensities by counting the clock numbers. Moreover, in order to improve the resolution of the ADC, we can increase the speed of the CLK.

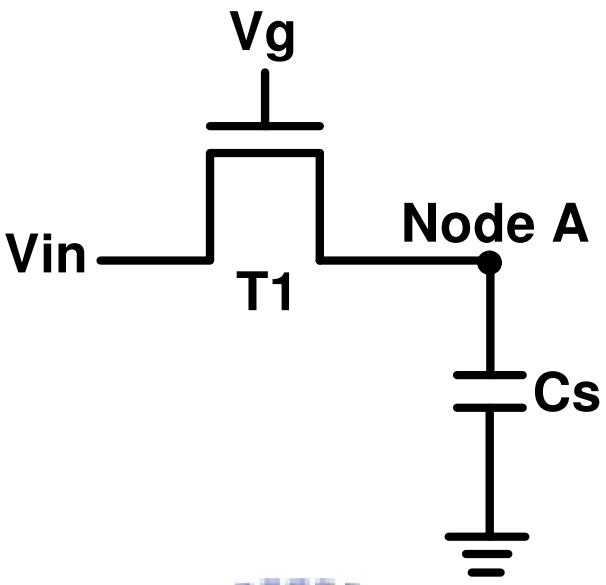

(a)

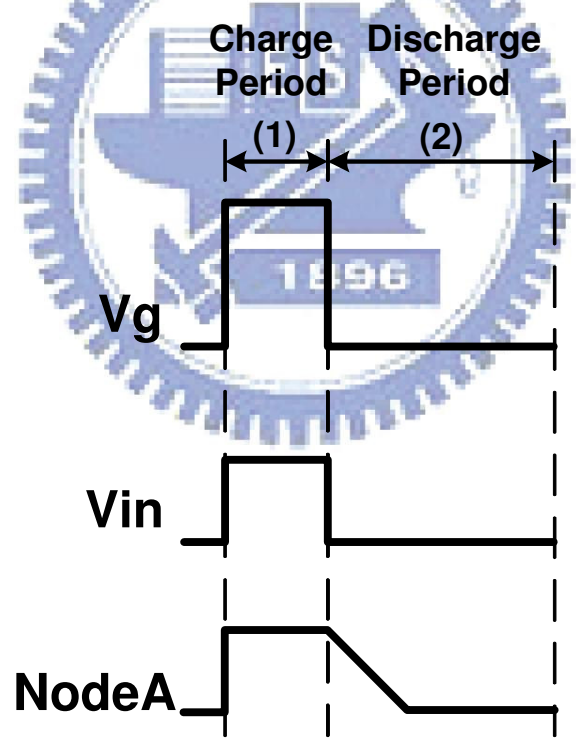

(b)

Fig. 3-1 (a) Schematic of proposed 1T1C light-sensing circuit and (b) timing sequence

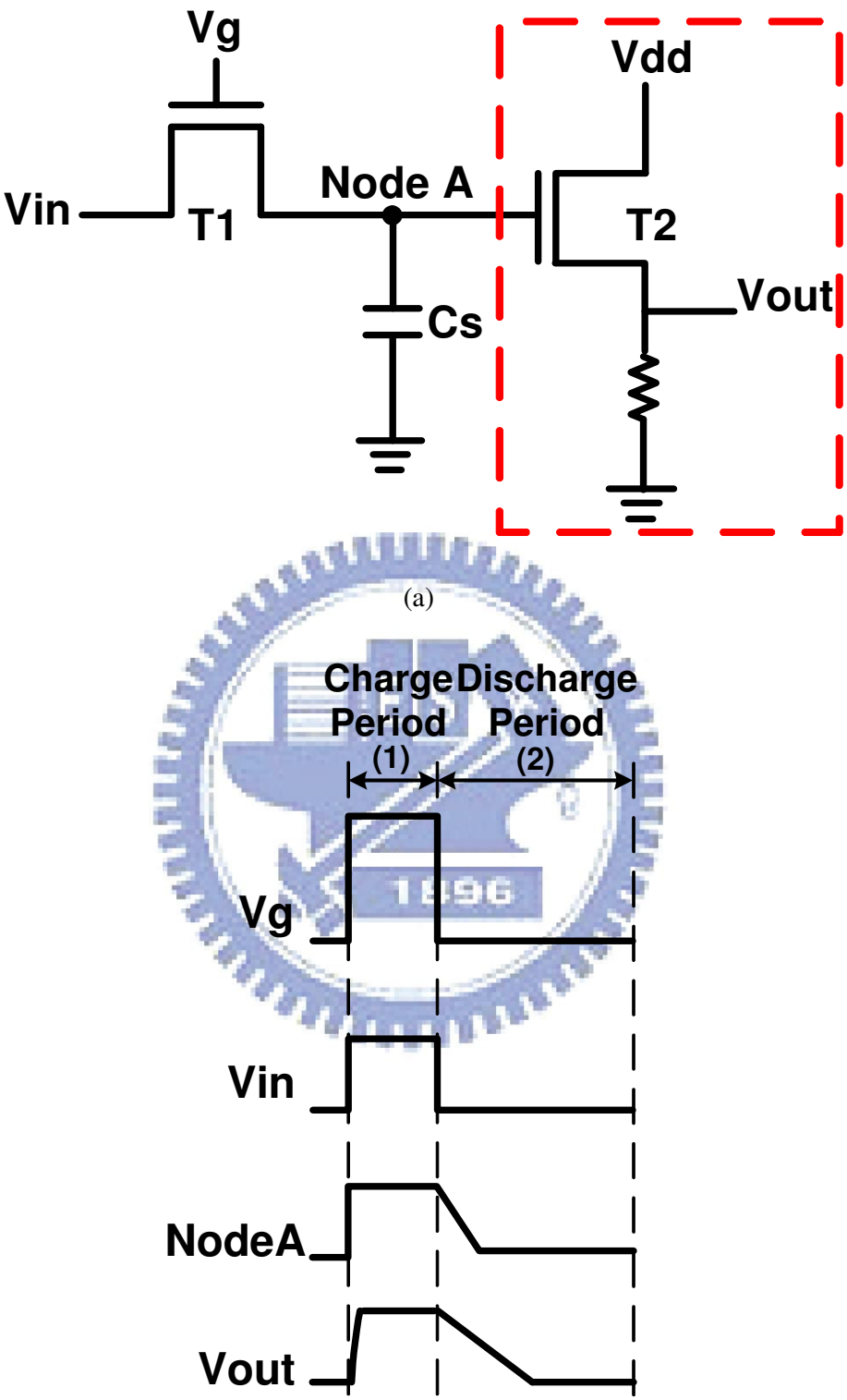

Fig. 3-2 (a) Schematic of proposed 2T1C light-sensing circuit and (b) timing sequence

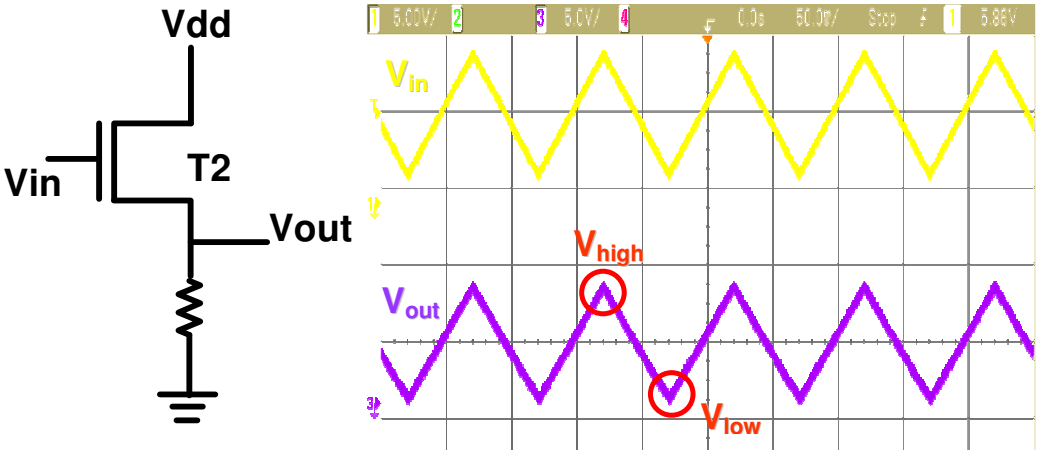

(a) (b)

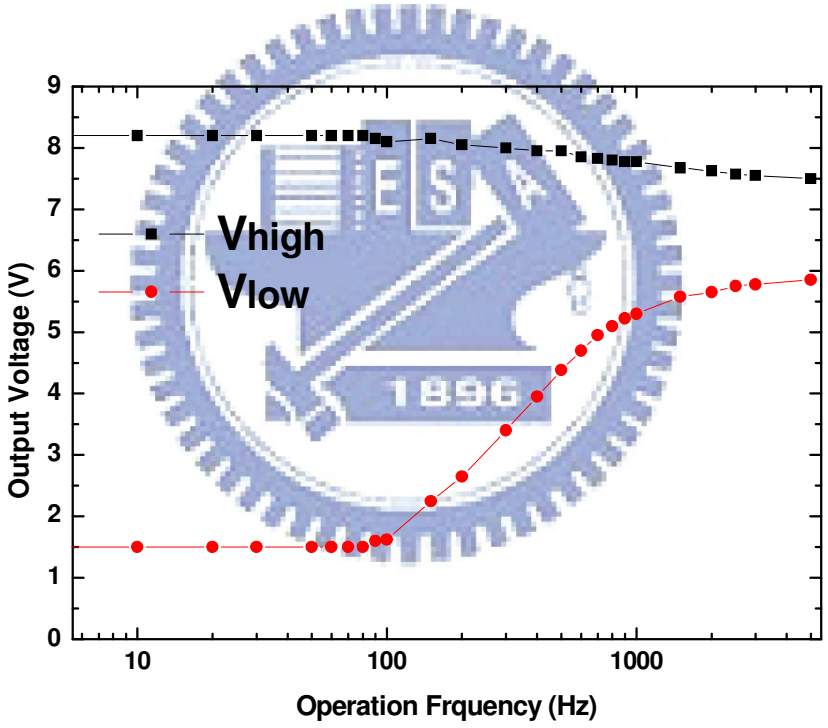

(c)

Fig. 3-3 (a) Schematic of conventional source follower (b) Wave form of the output signal when the input triangular signal is 2V to 9V (c) Frequency response of the source follower

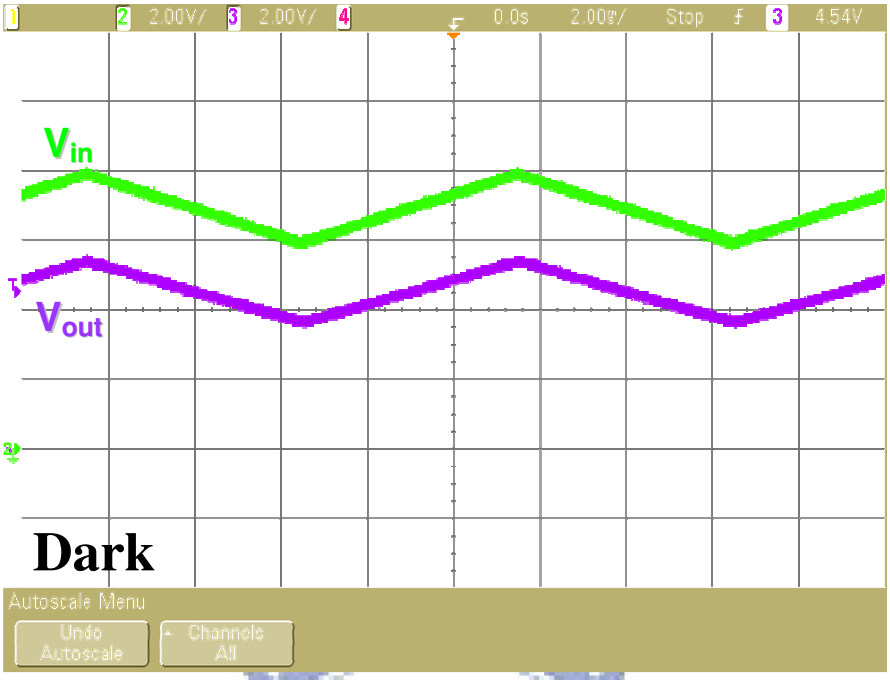

(a)

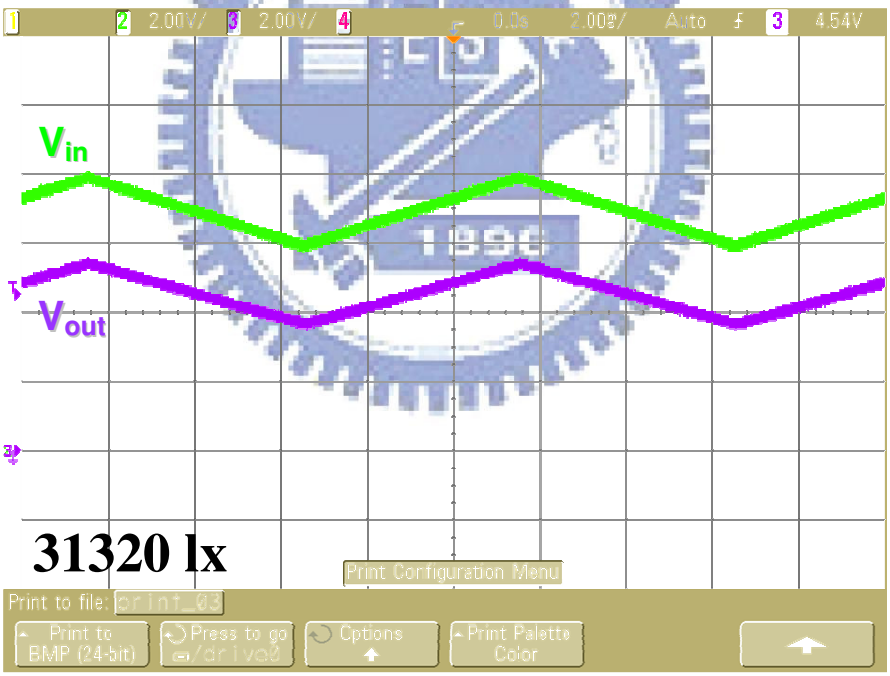

(b)

Fig. 3-4 The source follower input and output wave forms under (a) dark and (b) illuminated (31320 lx) conditions

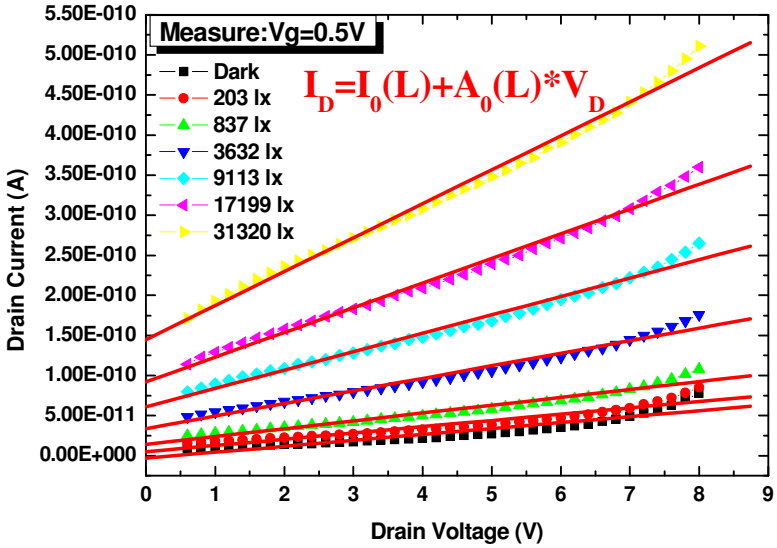

Fig. 3-5 Illumination dependence of I_D-V_D characteristic and its fitting formula

Table 3-1 $I_0(L)$ and $R_0 = 1/A_0(L)$ at V_{GS}=0.5V with the illumination intensity variation

Brightness	$I_0(L)$	$R_0=1/A_0(L)$
Dark	2.40E-12	1.81E+11
203lx	9.34E-12	1.58E+11
837lx	1.80E-11	1.18E+11
3632lx	3.82E-11	7.06E+10
9113lx	6.59E-11	4.71E+10
17199lx	9.80E-11	3.47E+10
31320lx	1.52E-10	2.50E+10

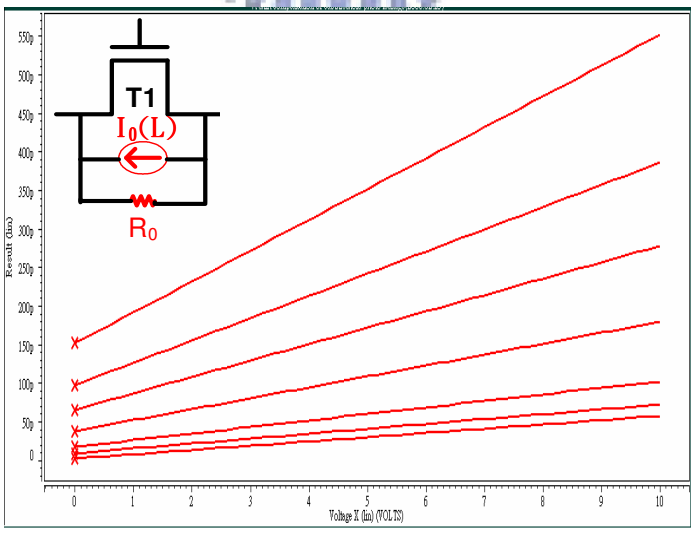

Fig. 3-6 SPICE simulation results of TFT (W/L=20um/5um)

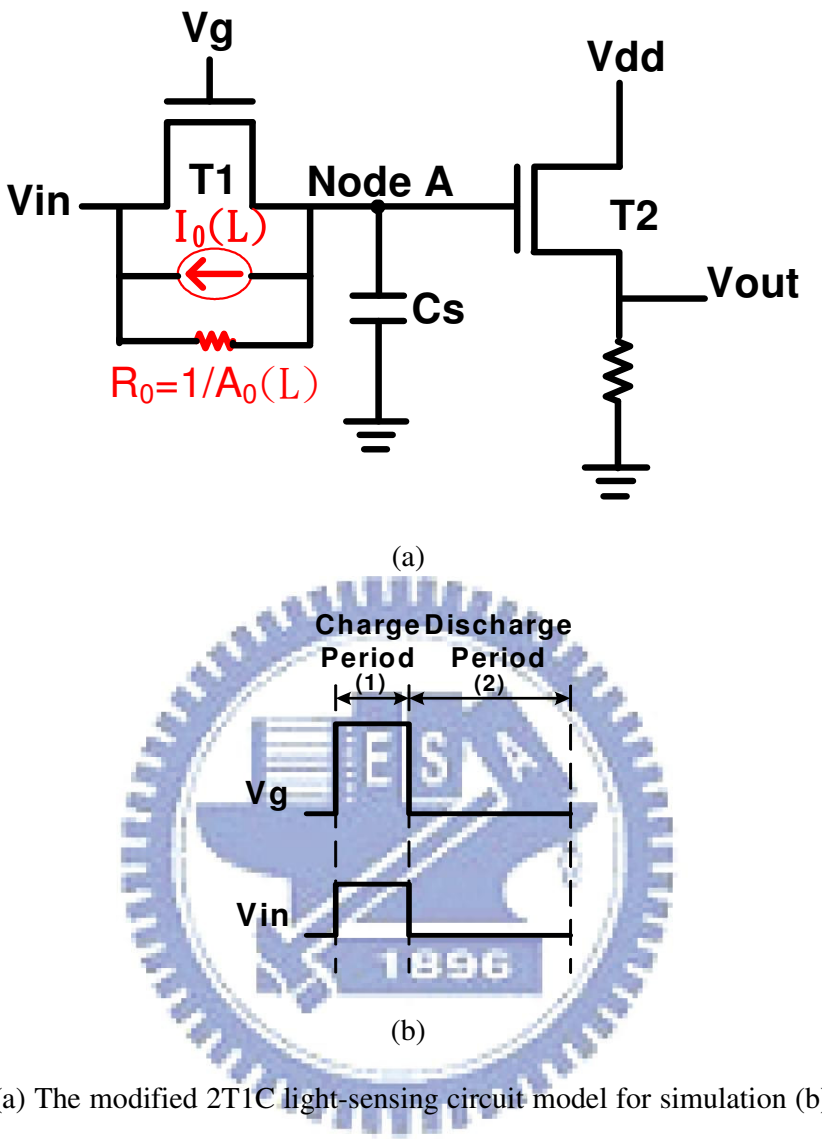

Fig. 3-7 (a) The modified 2T1C light-sensing circuit model for simulation (b) its time diagram.

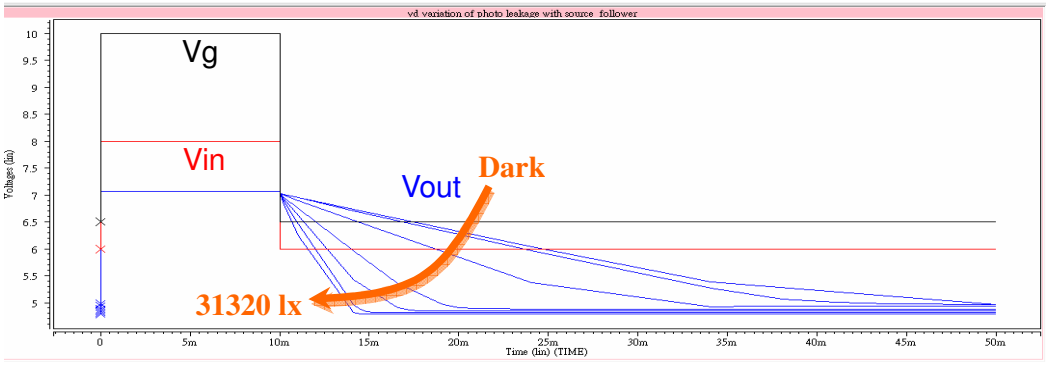

Fig. 3-8 Simulation results under illumination and in the dark

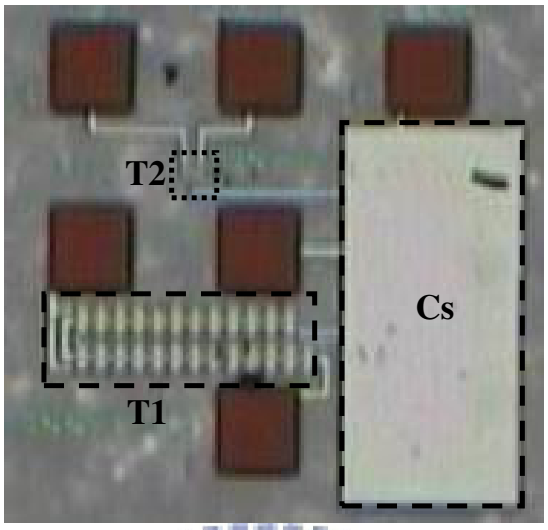

Fig. 3-9 Photograph of the fabricated 2T1C light-sensing circuit

Table 3-2 Experimental conditions

Feature	Specification	
Operation region	Sub. (V_{GS} = 0.5V)	OFF (V_{GS} = -2V)
Operation frequency	100 Hz	10 Hz
Illumination intensity	0~31320 lx	0~31320 lx
V_g	10V~6.5V	10V~4V
V_{in}	8V~6V	8V~6V
C_S	50 pF	20 pF
V_{DD}	10 V	10 V

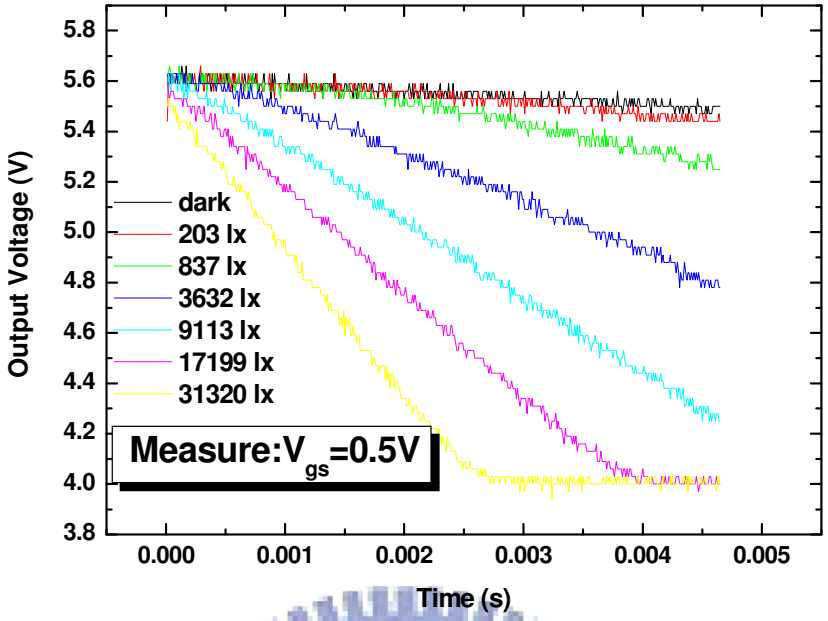

(a)

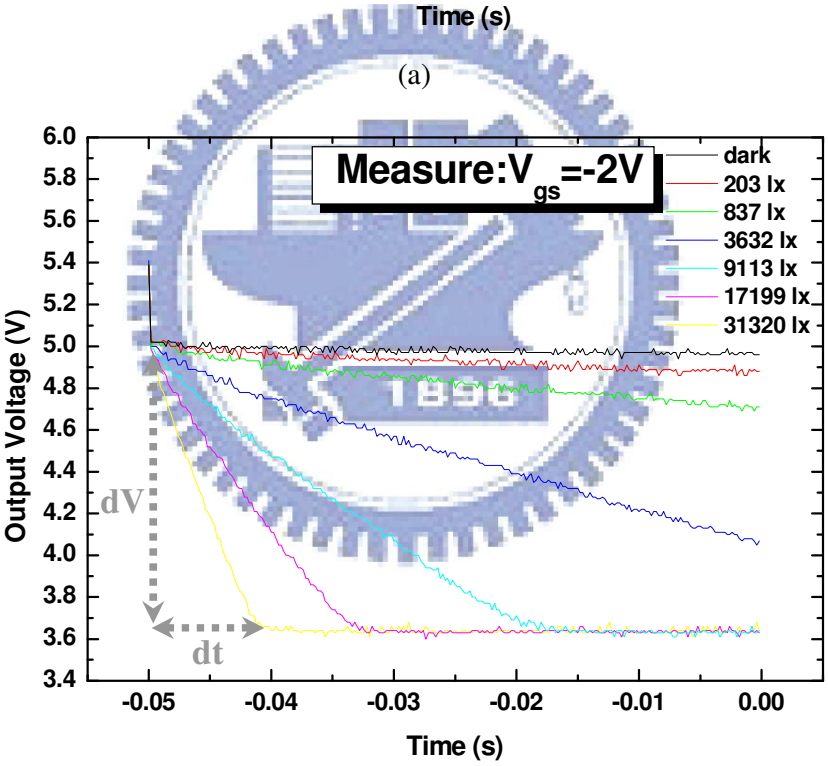

(b)

Fig. 3-10 Measured waveforms of output voltages of proposed 2T1C light-sensing circuit under halogen lamp illuminative variations from 0 to 31320 lx on (a) subthreshold region and (b) OFF region

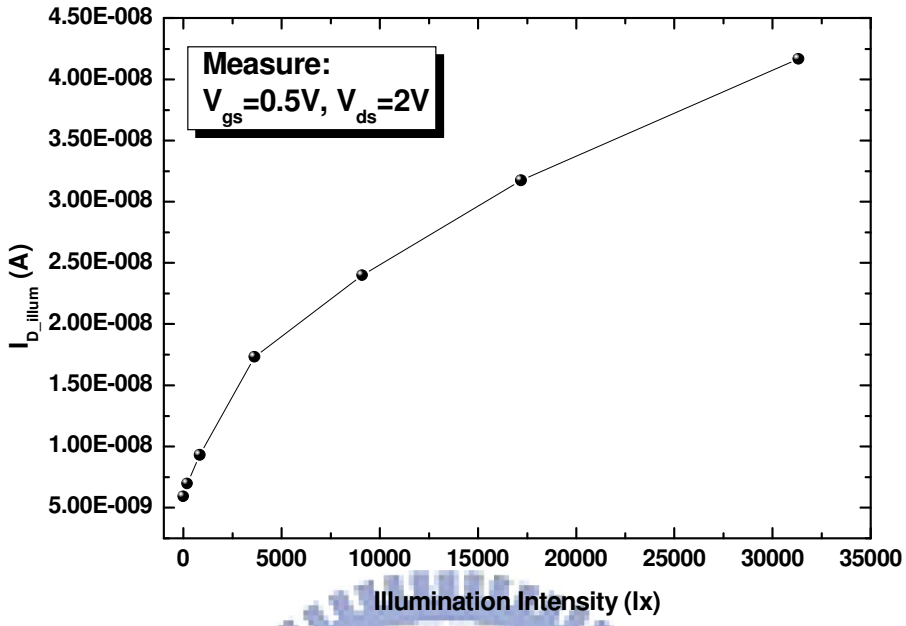

(a)

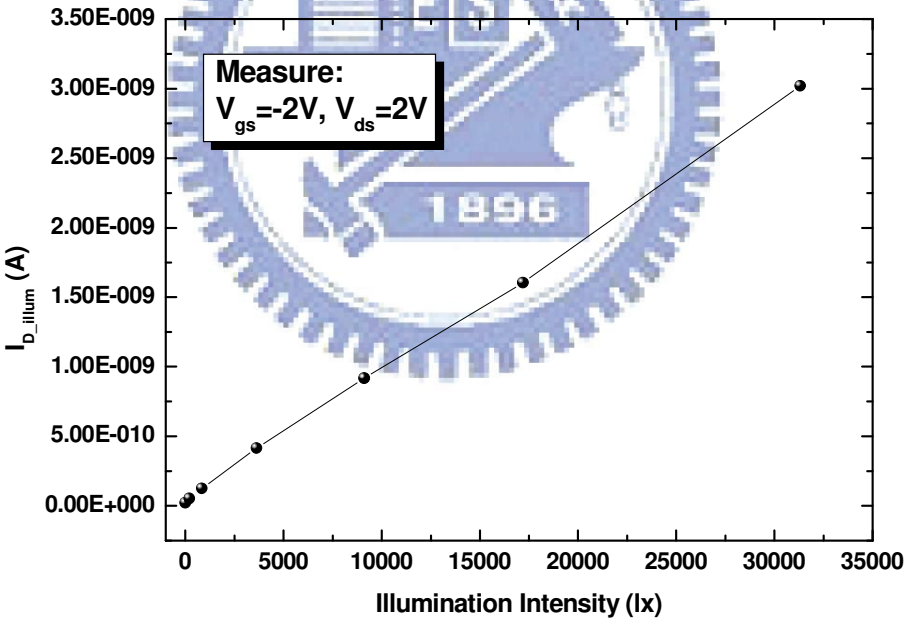

(b)

Fig. 3-11 Measurement results of the 2T1C circuit under different illumination intensity on (a) subthreshold region and (b) OFF region

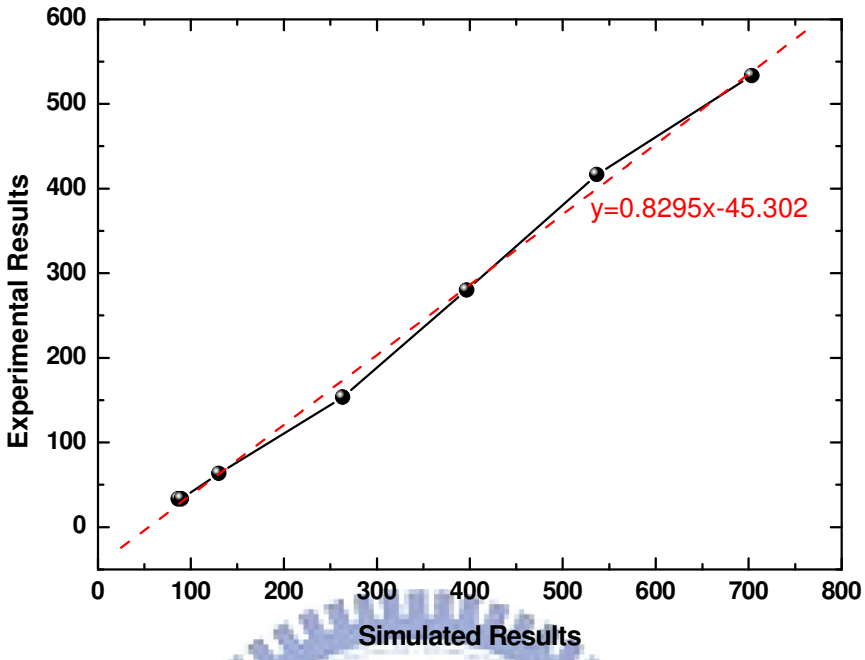

Fig. 3-12 Comparison with simulated & experimental results at V_{GS}=0.5V

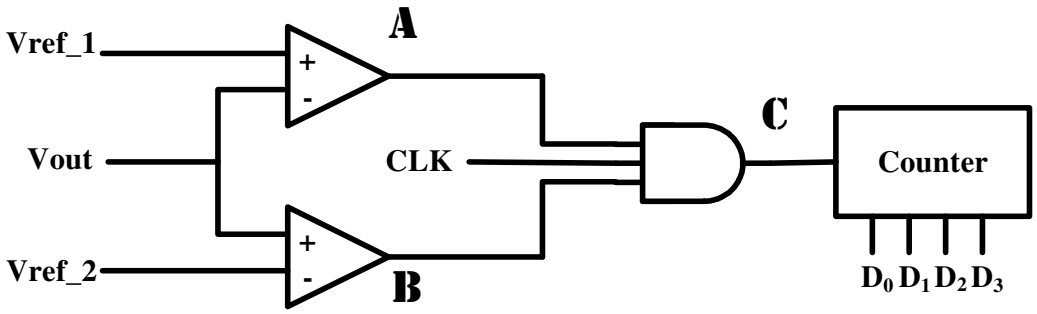

(a)

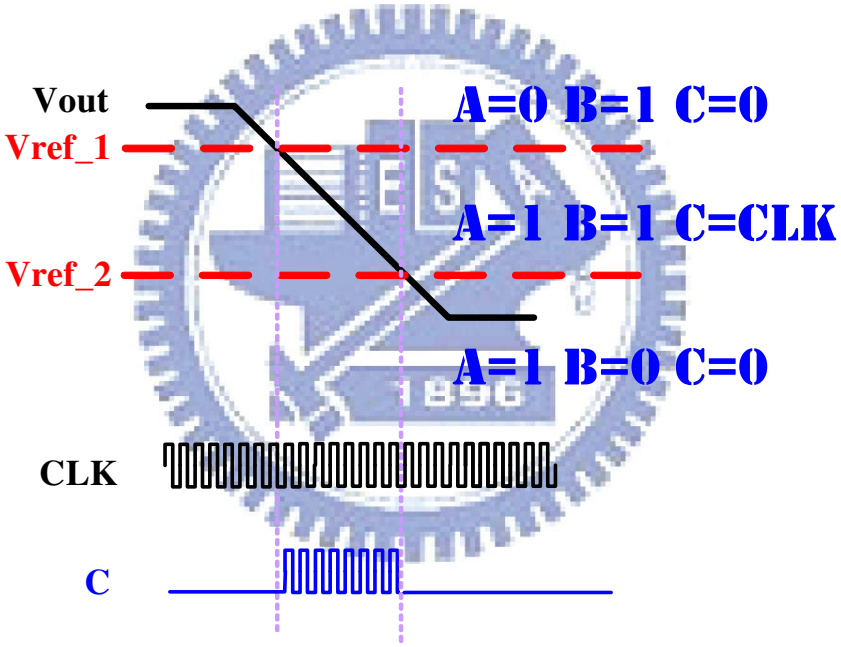

(b)

Fig. 3-13 (a) Simplified block diagram of digitization circuit and (b) its signal diagrams

Chapter 4

Assessment of LSC

4.1 Device Variation

It is clear that for any circuit to be manufacturable, device-to-device uniformity must be controlled. Qualitatively, the uniformity of LTPS TFTs is expected to be worse than that of MOS transistors made in single-crystal materials. This is because the TFTs are composed of grains, whose number, shape, and quality could vary from device to device. Even the devices fabricated under the identical process, LTPS TFTs still have different electrical characteristics due to the influence from different numbers of the inter-grain and intra-grain defects [19-20].

Figure 4-1 shows the transfer characteristic curves at V_{DS}=10V of 200 LTPS TFTs. Two of the differences are significant to the light-sensing circuit. One is threshold voltage (V_{th}) variation which is dominant in the subthreshold region and the other one is OFF current variation. As expected, the poly-Si TFTs are found to suffer from serious photosensitive device variation behavior which results from the diverse and complicated grain distribution in the poly-Si film, as shown in figure 4-2.

4.2 Error of LSC from Device Variation

Owing to these two kinds of device variation, the measured output voltages of our light-sensing circuit will deviate. It will cause an error while sensing image. We must ensure the accuracy of the circuit. Therefore, we have to discuss the impact of device variation on our photo sensor.

4.2.1 Threshold Voltage Shift

In order to take further steps to estimate the influence from V_{th} shift on the sensing results, we simulated the V_{th} shift by changing V_g low level. Figure 4-3 shows the influence of V_{th} shift ±0.3V based on V_{gs}=0.5V. We can see in this figure, only a little V_{th} shift would cause a significant deviation of output voltage in the subthreshold region, as expected. The measurement error is not controllable. On the other hand, we also considered the V_{th} shift in the OFF region, as shown in figure 4-4. We chose V_{gs}=-2V, -4V, -6V to bias the sensor in the OFF region, respectively. It is obvious that the impact of the V_{th} differences of the LTPS TFTs in the OFF region is slighter than that in the subthreshold region. As shown in figure 4-4 inset, the drain current is almost independent of the gate voltage under illumination in the OFF region except the case in the dark. For this reason, only the deviation of V_{th} difference for the sensor operating in subthreshold region is considered. We propose a V_{th} shift compensation to calibrate the error of our sensor in section 4.3.

4.2.2 OFF Current Variation

The measured output voltages in OFF region of fifteen proposed light-sensing circuits with respect to the illumination intensity are shown in figure 4-5. We can see the results are non-uniform. With the illumination intensity increase, the error becomes larger and larger. As discussed in section 4.2.1, it is almost independent of V_{th} difference. Therefore, OFF current variation is the dominant factor for the sensor operating in the OFF region. The deviation resulting from OFF current variation will cause a significant error of output voltage of our light-sensing circuit. In order to increase the photosensitivity, we also propose a method to calibrate the error of OFF current variation in next section.

4.3 Calibration Methods

To increase the photosensitivity of our light-sensing circuit to be practically used on LCD panels, we have to develop methods to calibrate the error of the circuit.

4.3.1 OFF Current Variation Calibration Method

After discussing the influence of OFF current variation as mention above, we have thought up a method to calibrate it. For the previous work in our lab (thesis of Yu-Te Chao), we try to use the statistical method to reduce the effect of OFF current variation [21]. Figure 4-6 shows the measured output voltages in OFF region of fifteen proposed light-sensing circuits on the same glass with respect to the illumination intensity and an average line of these results. Based on the average line, the error of illumination intensity is about 4700 lx and the signal to noise ratio is about 7. Where the signal to noise ratio is defined as following:

S/N=maximum illumination intensity/error.

In order to reduce the error of illumination intensity and increase the S/N ratio, we divided the fifteen samples into several groups, two samples, three samples, and five samples average for a unit. As shown in figure 4-7(a), figure 4-7(b), and figure 4-7(c), respectively, we can clearly see that the deviation is greatly reduced after calibration using statistical method. For further discussion, the error of the illumination intensity is reduced to 3200 lx, 2400 lx, and 1200 lx; and the S/N ratio is increased to 10, 13, and 26, respectively. The illumination intensity errors comparison between before and after calibration is summarized in Table 4-1. We also calculated the standard deviations versus the units that we divided above as shown in figure 4-8. In this figure, we believe that if we use more samples average for a unit, the resolution of our sensor can be even more improved.

4.3.2 Threshold Voltage Shift Compensation Circuit

In a LTPS TFT circuit, V_{th} non-uniformity is always a serious issue [22]. In addition to the initial V_{th} difference, the degradation of the driving TFTs by the lapse of operation time will cause V_{th} shift. Therefore, it is important to compensate the V_{th} shift variation [23-24]. Figure 4-9 shows the schematic of our proposed 4T2C light-sensing circuit with compensation part and its time diagram. The driving sequence consists of initialization period, compensation period, and sensing period including charge and discharge.

In the initialization period, when V_{in}, V_S, and Φ2 signals become "low" and V_g, Φ1 signals become "high", and thus T1 and SW1 turn on, and T2 and SW2 turn off. Because the C_{vt} is short when SW1 turn on and the voltages of V_A and V_S of C_S are equal, we can initialize the charges which stored in these two capacitors to be zero.

In the compensation period, when Φ1 and V_g signals become "low" and V_S signal becomes "high", and thus SW1 turns off. Based on the principle of charge conservation, V_B is equal to "V_{g_low}", V_A is equal to "V_{S_high}", and T1 turns off. At the same time, Φ2 signal becomes "high" and SW2 turns on. The voltage of V_B will charge to "V_{A_high}" and then T1 turns on again. At this time, V_A is discharged through T1 to "V_{in_low}" and V_B follows it till the voltages of V_A and V_B are equal to the threshold voltage of T1. Therefore, T1 turns off and the V_{th} is stored in the C_{vt}, where V_A and V_B can be expressed as

$$V_A = V_B = V_{th} - V_{g\_low}. \tag{10}$$

In the first half of sensing period (charge), when Φ2 and V_S signals become "low" and V_g signal becomes "high", the voltage of V_B will become "V_{g_high}+V_{th}-V_{g_low}" and T1 turns on again. V_{in} signal becomes "V_{in_high}" at the same time. Because we want to operate the sensor in the approximately linear region as

mentioned in section 3.4.1, we set the voltage of "V_{in_high}" to be small than 8V. Then the V_A, which is held by C_S, is charged to "V_{in_high}".

Finally, in the second half of sensing period (discharge), we want to operate the sensor in the subthreshold region, so the signal of V_g becomes "V_{g_sub}". Simultaneously, the signal of V_{in} becomes "V_{in_low}". Therefore, the V_A which is held by C_S is discharged by the photo leakage current of T1.

The proposed threshold voltage shift compensation circuit can overcome the variation due to V_{th} shift. Figure 4-10 and figure 4-11 show the fifty times of Monte Carlo simulation results of the proposed light-sensing circuit before and after compensation when V_{th} shift is ±0.5V. We can clearly see the variation is greatly reduced. Figure 4-12 shows the layout configuration of our threshold voltage shift compensation circuit. Because the fabricated sample is not ready for practical measurement, the V_{th} shift compensation operation and the output characteristic will verify in the future.

4.4 Application Assessment

After proposing some methods to calibrate the error of LSC from device variation as mention above, we assessed the application of our light sensor. If we want to use the circuit in ambient light sensor application, there is a problem to achieve this purpose. Because of the device variation, the resolution of the circuit can not satisfy this purpose. We should take further steps to improve the resolution of the LSC. On the other hand, we can use the circuit in touch panel application as long as using the 2T1C circuit with suitable storage capacitor we have mentioned in chapter 3 and operated it in the OFF region. We can integrate the circuit in pixel array. The LTPS photo sensor for touch panel application is possible.

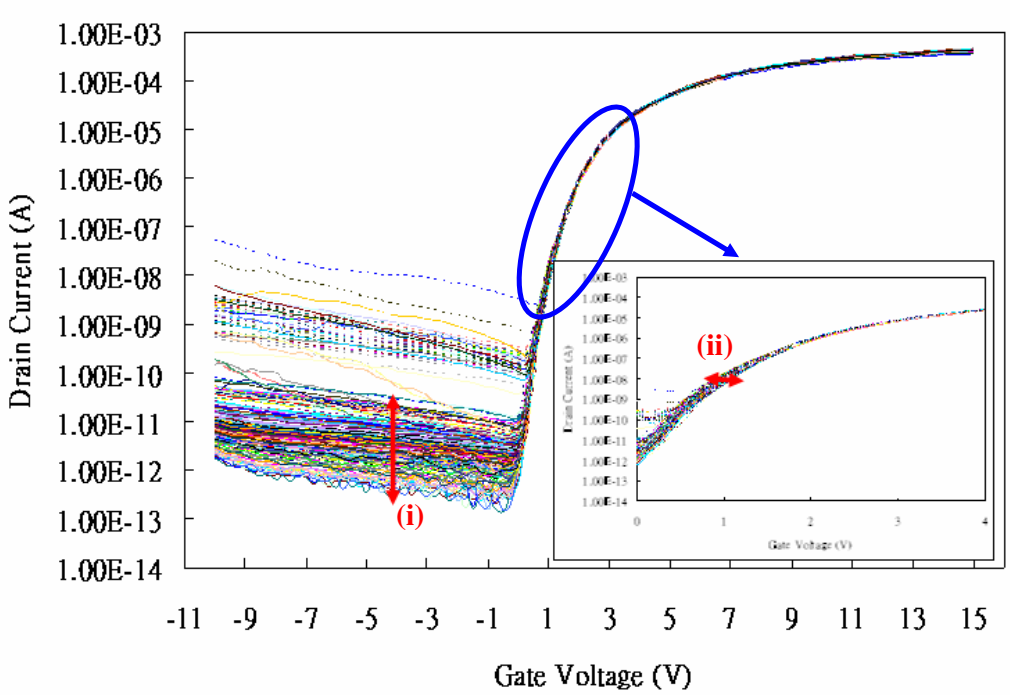

Fig. 4-1 The transfer characteristic curves of 200 LTPS TFTs at V_{DS}=10V: (i) initial OFF current variation (ii) threshold voltage shift

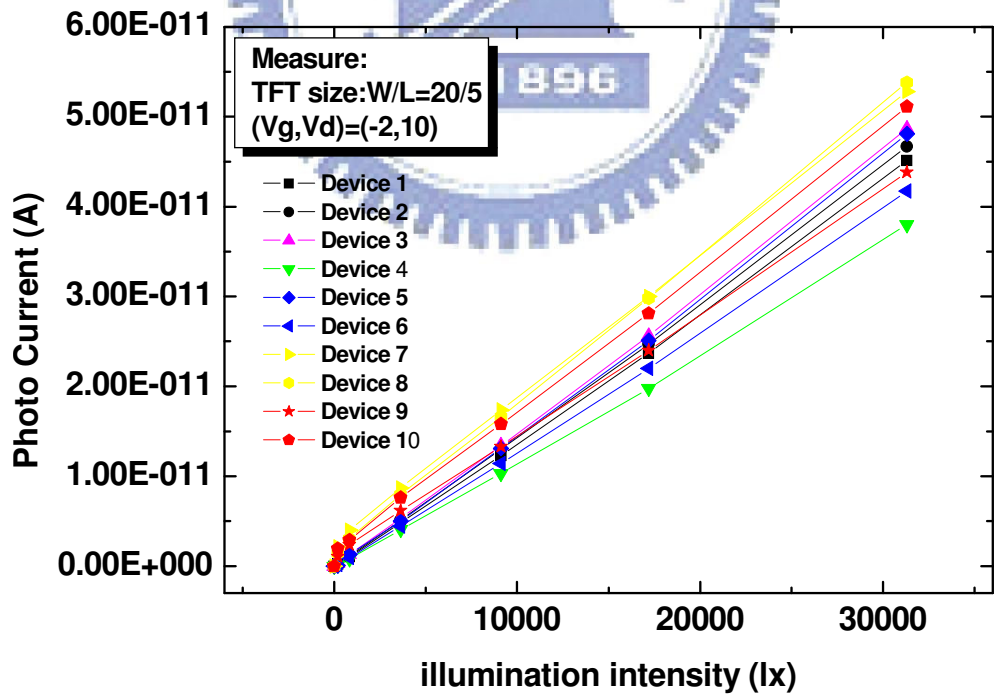

Fig. 4-2 Photo current variations of ten LTPS TFTs

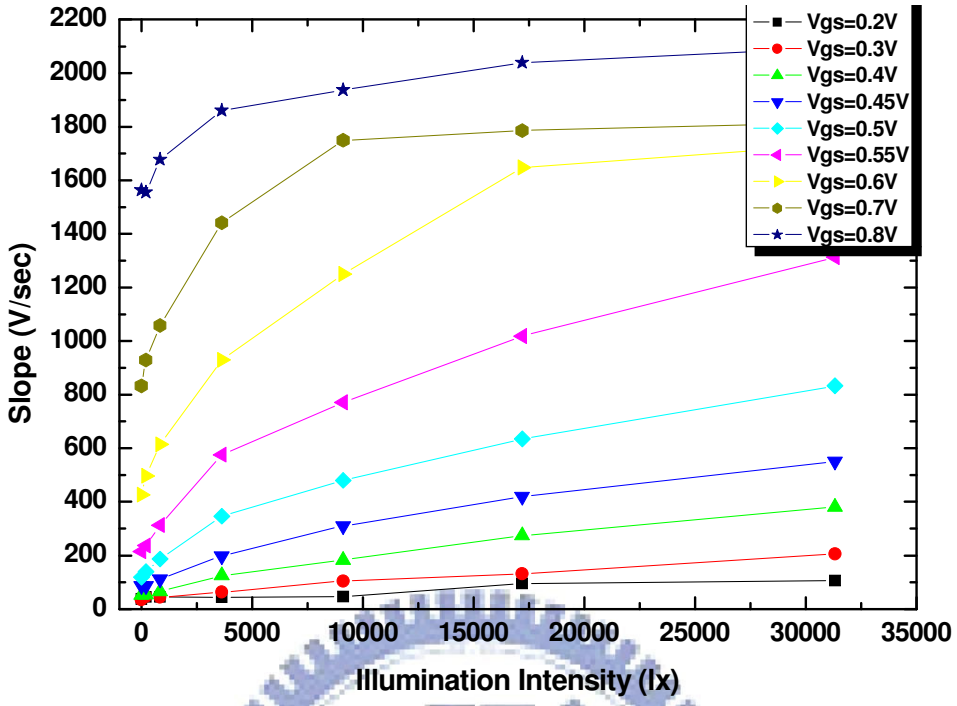

Fig. 4-3 The influence of V_{th} shift ±0.3V based on V_{GS}=0.5V (Operated in subthreshold region)

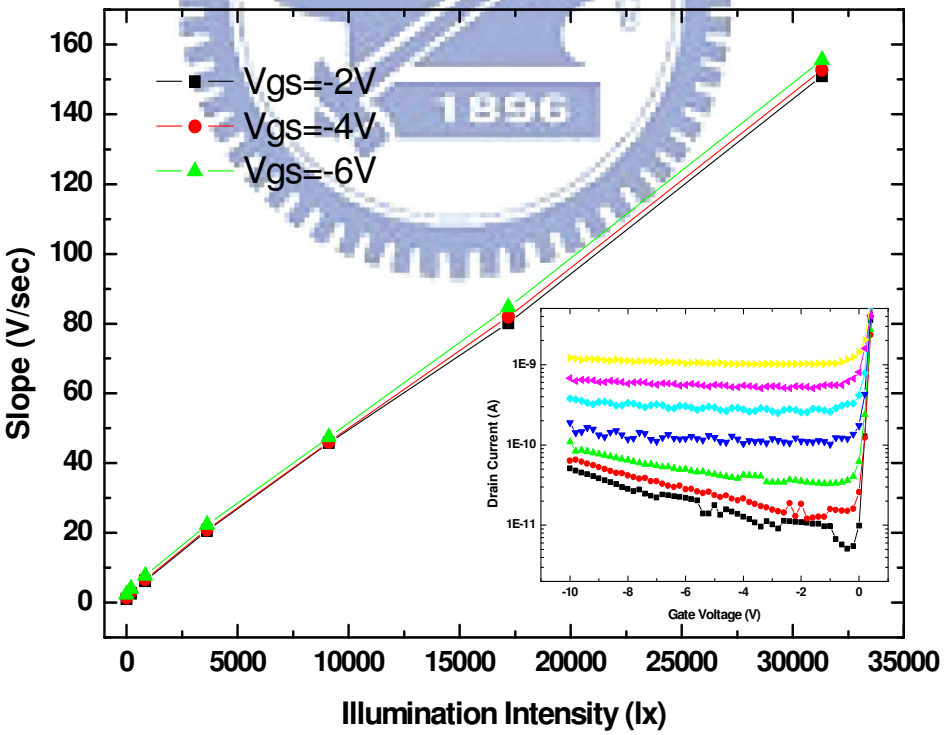

Fig. 4-4 The influence of V_{th} shift in OFF region

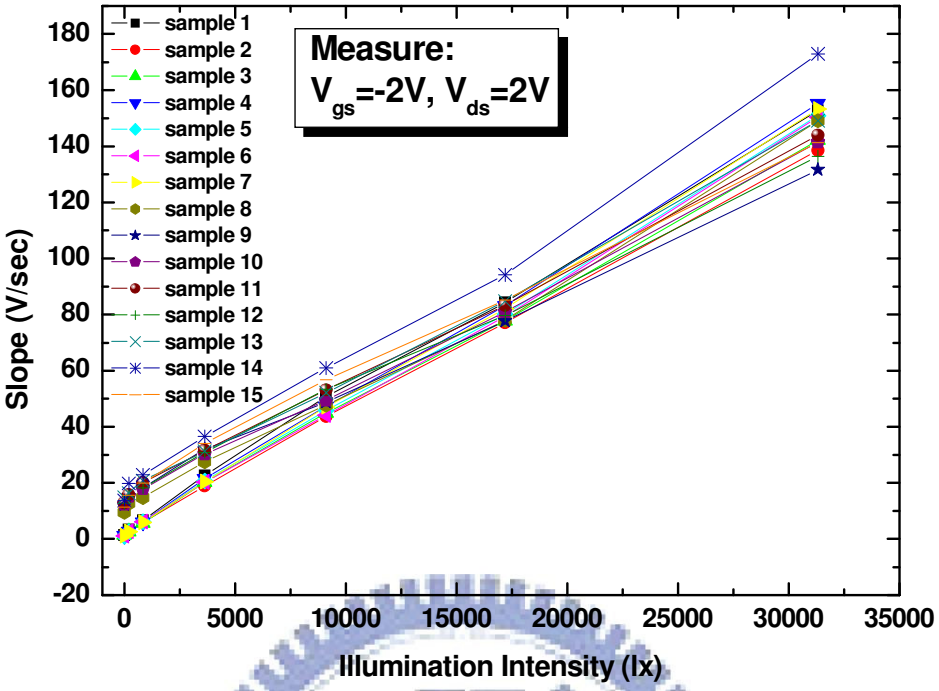

Fig. 4-5 Measured output slopes of fifteen proposed light-sensing circuits in OFF region

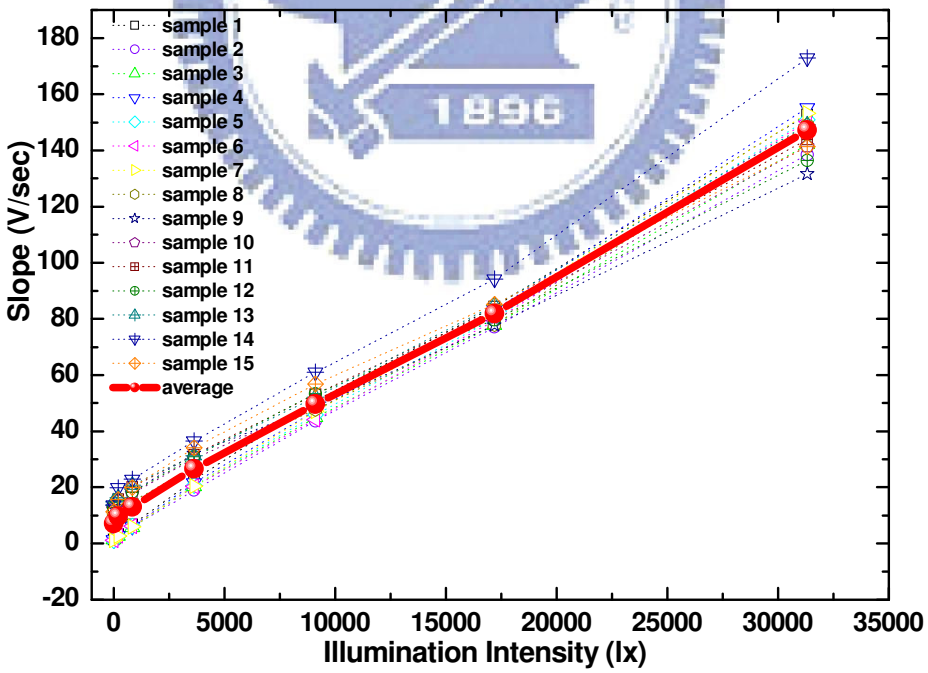

Fig. 4-6 Measured output slopes of fifteen proposed light-sensing circuits in OFF region (dash line) and their average curve (solid line)

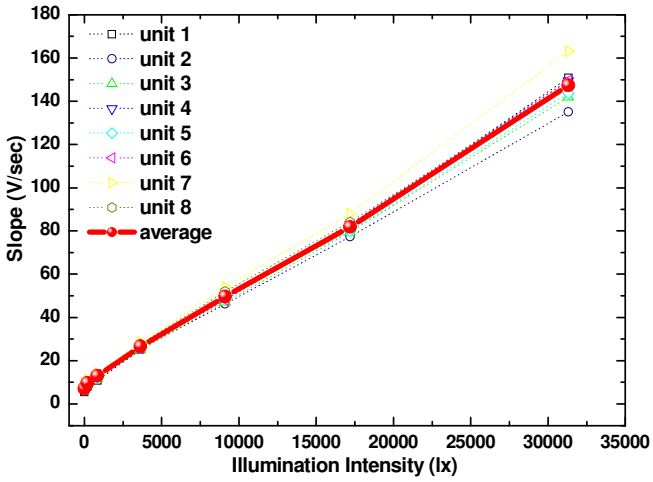

(a)

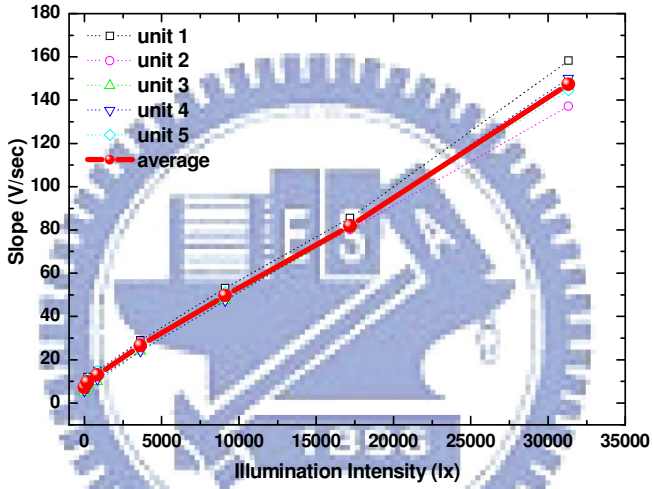

(b)

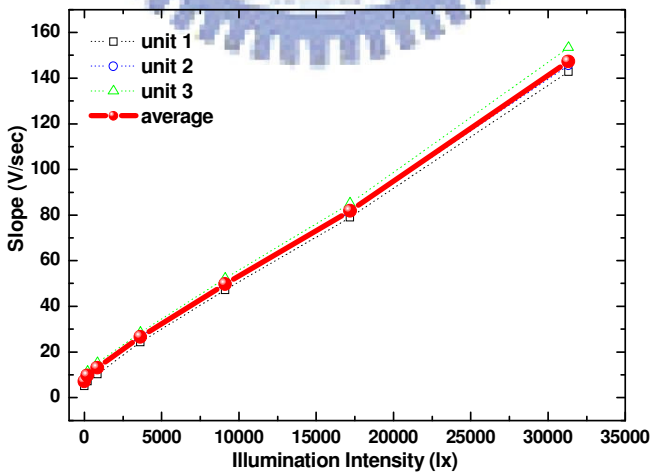

(c)

Fig. 4-7 Divided the fifteen samples into several groups: (a) two samples average for a unit, (b) three samples average for a unit, and (c) five samples average for a unit

Table 4-1 Comparison Results

Comparison		Error (lx)	S/N	Corresponding Digitized Resolution
Before Calibration		4700	7	3 bits
After Calibration	2 for a unit	3200	10	4 bits
	3 for a unit	2400	13	
	5 for a unit	1200	26	5 bits

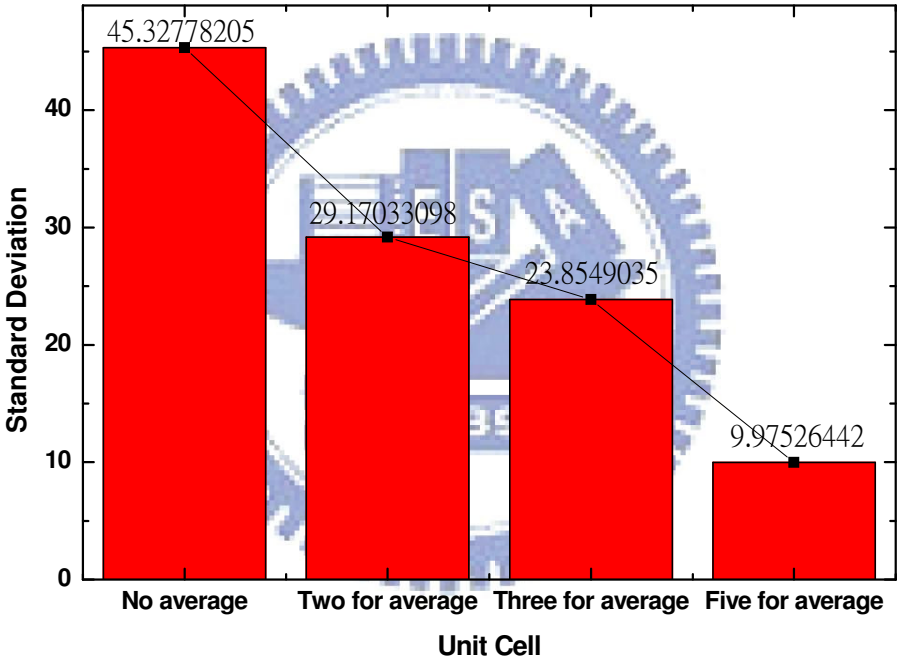

Fig. 4-8 Standard deviations versus the units

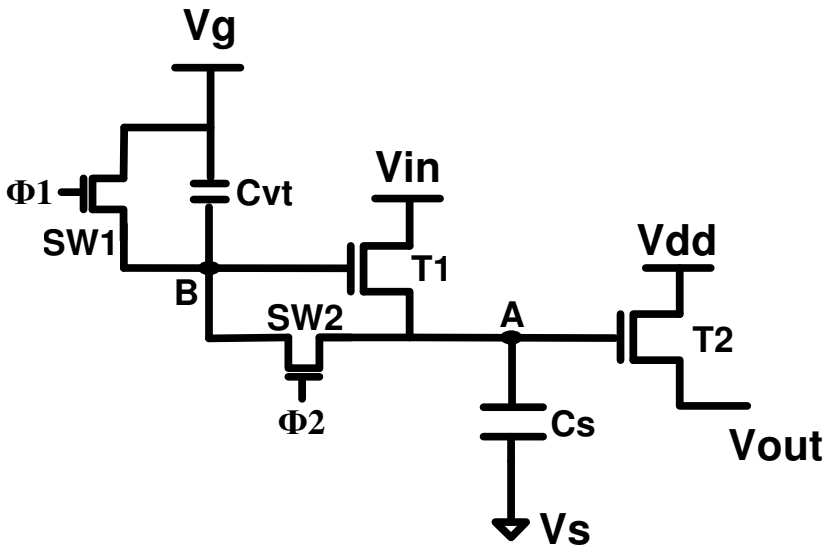

(a)

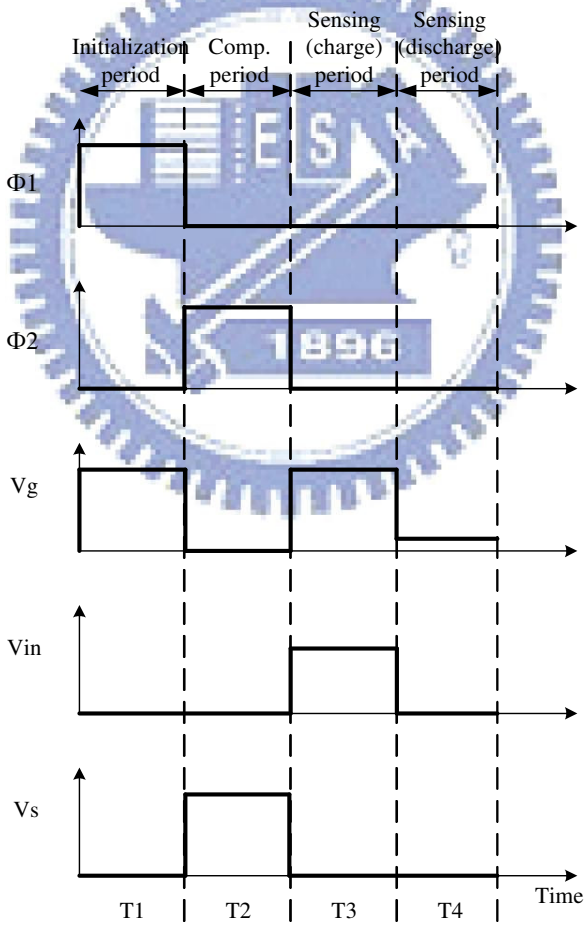

(b)

Fig. 4-9 (a) Schematic of our proposed light-sensing circuit with compensation part and (b) time diagram

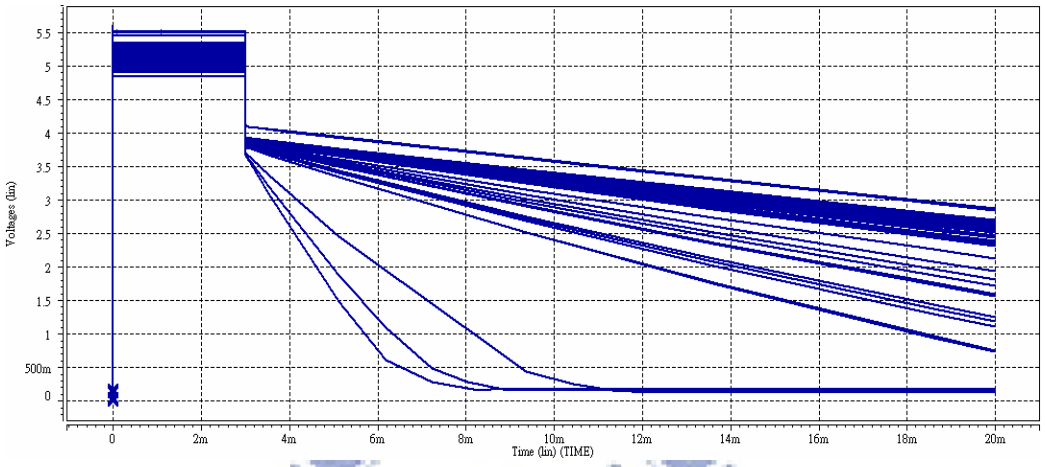

(a)

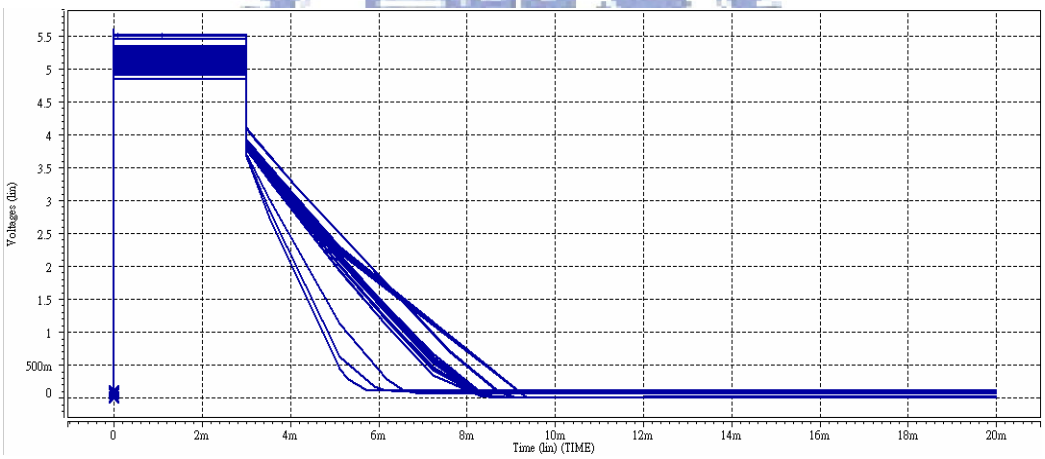

(b)

Fig. 4-10 Fifty times of Monte Carlo simulation results of the proposed 2T1C light-sensing circuit when V_{th} shift is ±0.5V (a) in the dark and (b) under 31320 lx illumination intensity

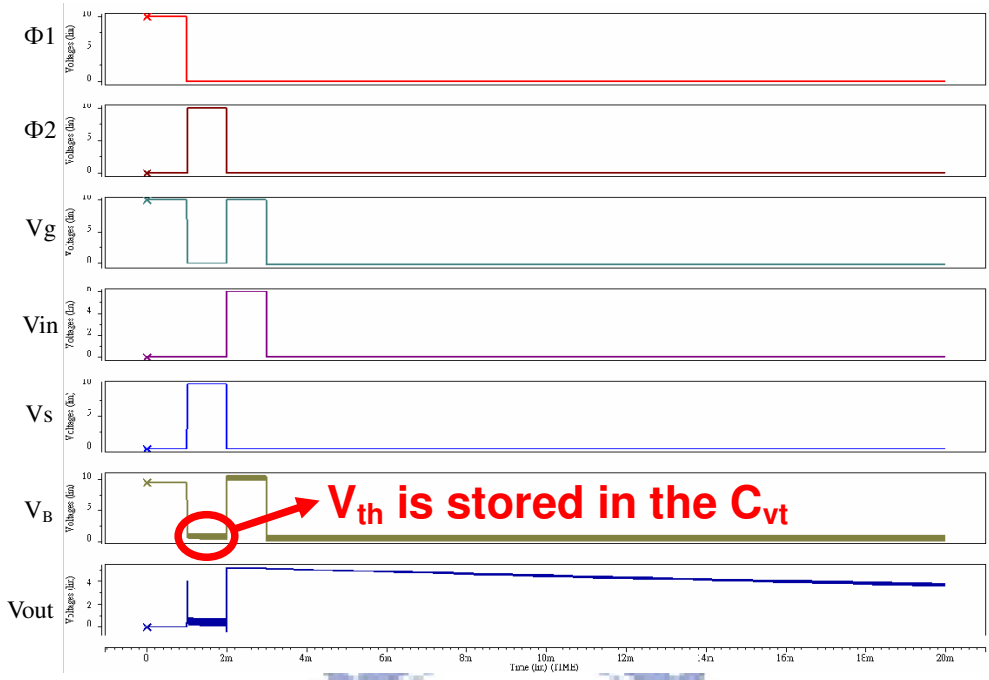

(a)

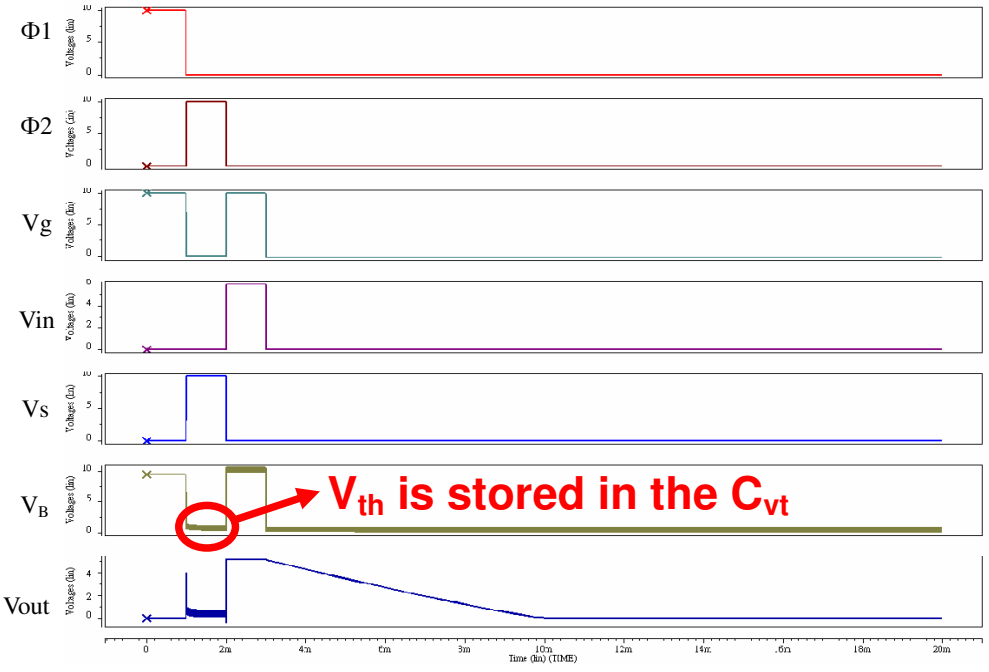

(b)

Fig. 4-11 Fifty times of Monte Carlo simulation results of the proposed 4T2C light-sensing circuit when V_{th} shift is ±0.5V (a) in the dark and (b) under 31320 lx illumination intensity

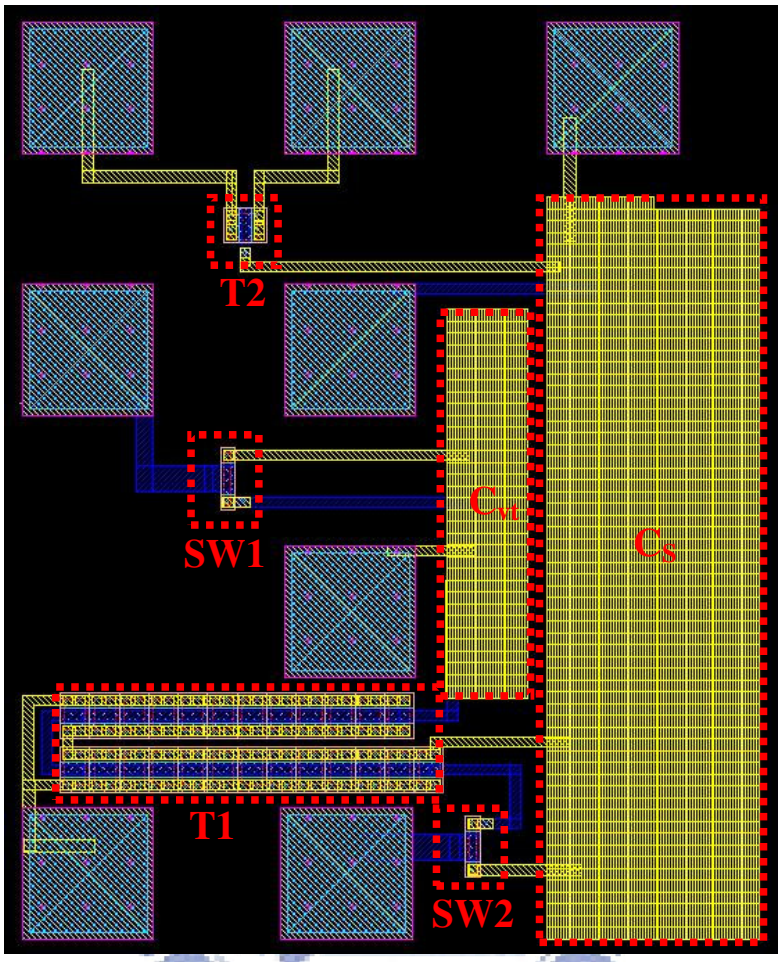

Fig. 4-12 Layout configuration of our threshold voltage shift compensation circuit

Chapter 5

Conclusions

In this thesis, a newly developed light-sensing circuit using the identical LTPS TFTs fabrication processes has been proposed. The proposed circuit, which has a source follower part, can perform not only sensing operation but also trustworthy readout operation through amplifying small photo leakage current to analog voltage. As experimental results show, due to the poor uniformity of LTPS TFTs, we also proposed the calibration methods to reduce the illumination intensity error from 4700lx to 1200lx and compensate the V_{th} shift variation.

In our research, we study on the feasibility of LTPS TFTs for light sensing application; we also have presented a detailed experimental study of the LTPS TFTs behavior and identified the different TFT operating regimes under halogen illumination. It can operate in either subthreshold region or OFF region to sense the photo current but need to trade off. Table 5-1 shows the merits and drawbacks of these two operating regimes, respectively. Although the current level of subthreshold region is larger than that of OFF region, it is not suitable for light sensing application due to the drawbacks of nonlinear dependence with illumination intensity and strongly dependence with gate voltage. A slight shift could result in erroneous values. We therefore believe that it should be used to detect the presence of light in subthreshold region. The OFF region would be more appropriate for the purpose that is to accurately quantify the light intensity. We also consider the back light effect and figure it out that the back light effect can be subsided during sensing period. Therefore, we think that the LTPS photo sensor for touch panel is possible.

Table 5-1 Merits and drawbacks of Sub. region & OFF region

	Merit	Drawback
Sub. Region	1. Large current level 2. Short response time	1. Small photosensitivity 2. Nonlinear dependence with irradiation intensity 3. Strongly dependence with gate voltage
OFF Region	1. Large photosensitivity 2. Linear dependence with irradiation intensity 3. Almost independent of gate voltage	1. Small current level 2. Large response time

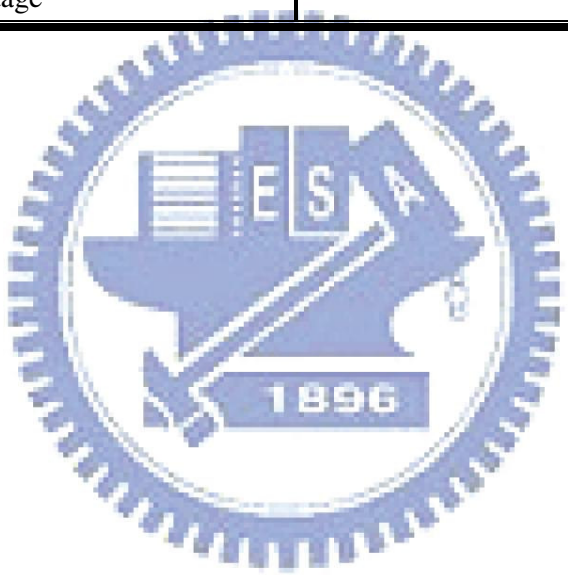

References

[1] Y.Nakajima, “Latest Development of System-on-Glass Displays using Low Temperature Poly-Si TFT, ” Journal of the Society for Information Display, Vol. 12, n4, pp.361-365, 2004

[2] H. Ohshima, M. Fuhren, “High-Performance LTPS Technologies for Advanced Mobile Display Applications,” SID’07 Symposium Digest, pp.1482-1485, 2007

[3] T. Nakamura *et al*, “TFT-LCD with Image Capture Function using LTPS Technology,” IDW’03, pp.1661, 2003

[4] M. Kimura, T. Shima, T. Okuyama, S. Utsunomiya, W. Miyazawa, S. Inoue, T. Shimoda, “Artificial Retina using Thin-Film Transistors,” AM-LCD’05, pp.323-326, 2005

[5] K. Maeda, T. Nagai, T. Sakai, N. Kiwabara, S. Nishi, M. Satoh, T. Matsuo, S. Kamiya, H. Katoh, M. Ohue, Y. Kubota, H. Komiya, T. Muramatsu, M. Katayama, “The system-LCD with Monolithic Ambient-Light Sensor System,” SID’05 Symposium Digest, pp.356-359, 2005

[6] S. Koide, S. Fujita, S. Fujikawa, T. Matsumoto, “LTPS Ambient Light Sensor with Temperature Compensation,” IDW’06 Digest, pp.689-690, 2006

[7] Y-M. Tsai, D-Z. Peng, C-W. Lin, C-H. Tseng, S-C. Chang, PY. Lu, L-J. Chen, H-L. Hsu, R. Nishikawa, “LTPS and AMOLED Technologies for Mobile Displays,” SID’06 Symposium Digest, pp.1451-1454, 2006

[8] A-W. Wang, K-C. Saraswat, “A Strategy for Modeling of Variations due to Grain Size in Polycrystalline Thin-Film Transistors,” IEEE Transactions on Electron Devices, Vol. 47, n5, pp.1035-1043, 2000

[9] J-D. Gallezot, S. Martin, J. Kanicki, “Photosensitivity of a-Si:H TFTs,” IDW’01 Asia Display, pp.407-410, 2001

[10] N. Tada, H. Hayashi, M. Yoshida, M. Ishikawa, T. Nakamura, T. Motai, T. Nishibe, “A Touch Panel Function Integrated LCD Using LTPS Technology,” IDW’04, pp.349-350, 2004

[11] H. Hayashi, T. Nakamura, N. Tada, T. Imai, M. Yoshida, H. Nakamura, “Optical Sensor Embedded Input Display Usable under High-Ambient-Light Conditions,” SID’07 Symposium Digest, pp.1105-1108, 2007

[12] K. Kobayashi, Y. Niwano, “Photo-Leakage Current of Poly-Si Thin Film Transistors with Offset and Lightly Doped Drain Structure,” Jpn. J. Appl. Phys. Vol. 38, pp.5757-5761, 1999

[13] F. Matsuki, K. Hashimoto, K. Sano, D. Yeates, J. R. Ayres, M. Edwards, A. Steer, “Integrated Ambient Light Sensor in LTPS AMLCDs,” SID’07 Symposium Digest, pp.290-293, 2007

[14] N.P. Papadopoulos, A.A. Hatzopoulos, D.K. Papakostas, C.A. Dimitriadis, S. Siskos, “Modeling the Impact of Light on the Performance of Polycrystalline Thin-Film Transistors at the Sub-threshold Region,” Microelectronics Journal, Vol. 37, pp.1313-1320, 2006

[15] W. den Boer, A. Abileah, P. Green, T. Larsson, S. Robinson, T. Nguyen, “Active Matrix LCD with Integrated Optical Touch Screen,” SID’03 Symposium Digest, pp.1494-1497, 2003

[16] A. Abileah, W. den Boer, T. Larsson, T. Baker, S. Robinson, R. Siegel, N. Fickenscher, B. Leback, T. Griffin, P. Green, “Integrated Optical Touch Panel in a 14.1” AMLCD,” SID’04 Symposium Digest, pp.1544-1547, 2004

[17] B-T. Chen, Y-H. Tai, Y-J. Wei, K-F. Wei, C-C. Tsai, C-Y. Huang, Y-J. Kuo, H-C. Cheng, “Investigation of Source-Follower type Analog Buffer using Low Temperature Poly-Si TFTs,” Solid-State Electronics, Vol. 51, pp.354-359, 2007

[18] G-Y. Yang, Y-G. Kim, T-S. Kim, J-T. Kong, “S-TFT: An Analytical Model of

Polysilicon Thin-Film Transistors for Circuit Simulation, ” IEEE Custom Integrated Circuits Conference, pp.213-316, 2000

[19] Y. Kitahara, S. Toriyama, N. Sano, “A New Grain Boundary Model for Drift-Diffusion Device Simulations in Polycrystalline Silicon Thin-Film Transistors,” Jpn. J. Appl. Phys. Vol. 42, n6, pp.634-636, 2003

[20] C. Michael, M. Ismail, “Statistical Modeling for Computer-Aided Design of MOS VLSI Circuits,” Amsterdam, The Netherlands: Kluwer Academic, pp.8-10, 1993

[21] Y-H. Tai, S-C. Huang, W-P. Chen, Y-T. Chao, Y-P. Chou, G-F. Peng, “A Statistical Model for simulating the Effect of LTPS TFT Device Variation for SOP Applications,” IEEE Journal of Display Technology, Vol. 3, pp.426-433, 2007

[22] S-K. Hong, B-K. Kim, Y-M. Ha, “LTPS Technology for Improving the Uniformity of AMOLEDs,” SID’07 Symposium Digest, pp.1366-1369, 2007

[23] A. Nathan, G-R. Chaji, S-J. Ashtiani, “Driving Schemes for a-Si and LTPS AMOLED Displays,” IEEE Journal of Display Technology, Vol. 1, n2, pp.267-277, 2005

[24] H-S. Lim, O-K. Kwon, “Ambient Light Sensing Circuit with Low-Temperature Polycrystalline Silicon p-Intrinsic-n Diode and Source Follower for Auto Brightness Control,” Jpn. J. Appl. Phys. Vol. 47, n3, pp.1919-1923, 2008